NOTA TÉCNICA 4
Área de Evaluación y Modelización del Cambio Climático

Climate model validation in the Euro-Atlantic domain using Circulation Types

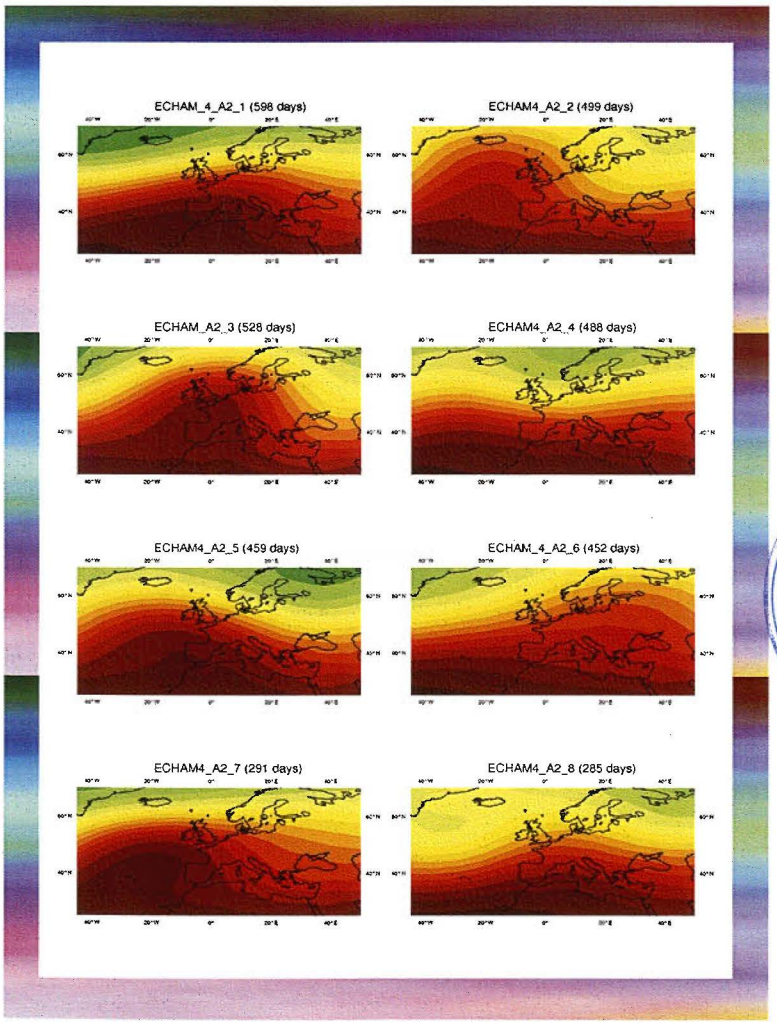

M. A. Pastor, M. J. Casado y F. J. Doblas-Reyes

GOBIERNO DE ESPAÑA
MINISTERIO DE MEDIO AMBIENTE Y MEDIO RURAL Y MARINO
AEMet Agencia Estatal de Meteorología

NT AEMCC 4

CLIMATE MODEL VALIDATION IN THE EURO-ATLANTIC DOMAIN USING CIRCULATION TYPES

M. A. Pastor [1], M. J. Casado [1], F. J. Doblas-Reyes [2]

(1) Agencia Estatal de Meteorología, Madrid, Spain
(2) European Centre for Medium-Range Weather Forecasts, Reading, UK

AGENCIA ESTATAL DE METEOROLOGÍA

GOBIERNO DE ESPAÑA
MINISTERIO DE MEDIO AMBIENTE, Y MEDIO RURAL Y MARINO
AEMet Agencia Estatal de Meteorología

2008

Acknowledgements:

The authors acknowledge the scientists involved in producing the ERA40 re-analyses and CGCM2, ECHAM4 and HADCM3 climate simulations. FJDR was supported by the EU-funded ENSEMBLES project (GOCE-CT-2003-505539).

Catálogo de publicaciones oficiales
http://www.060.es

Nota Técnica 4 del Área de Evaluación y Modelización del Cambio Climático (NT AEMCC-4)
Agencia Estatal de Meteorología

Edita: Centro de Publicaciones
Secretaría General Técnica
Ministerio de Medio Ambiente, y Medio Rural y Marino ©

ISBN: 978-84-8320-478-8
NIPO: 770-08-141-3
Depósito Legal: M-52874-2008
Imprime: Imprenta de la Agencia Estatal de Meteorología

Index

Abstract

In the present study the mid-tropospheric circulation of the re-analysis produced by the European Centre for Medium-Range Weather Forecasts and of three climate models from the Third Assessment Report (TAR) of the Intergovernmental Panel on Climate Change (IPCC,2001) has been analyzed. The analysis is based on a circulation-type approach, with principal component analysis in T-mode, followed by a rotation varimax procedure. This study has been performed over the Euro-Atlantic region and for the extended winter season.

A set of circulation types obtained has been identified and described in terms of their spatial features, frequency of occurrence, persistence, trends and transitions. The inter-annual variation of the circulation types is very high. The less frequent circulation type is connected with tilted ridges approaching Iberia whereas the most frequent ones are linked to the zonal regime or ridges from Iberia to Scandinavia.

The response of the atmospheric circulation when considering a future scenario, (IPCC SRES A2) is, in general, model dependent, showing a different behaviour with respect to the control simulation, especially as far as the number of 1-day events and the mean duration is considered. There are preferred paths for transitions between specific circulation types, especially the transition from a ridge stretching from Iberia to Scandinavia to a strong zonal flow.

It is concluded that the circulation types approach is a useful tool to validate climate models.

1. INTRODUCTION

The reliable simulation of continental-scale circulation by global circulation models (GCMs) is a necessary, though by far not sufficient, condition for assessing climate change impacts successfully. Although the location of major centres of action appears to be simulated relatively well by most models (Gates *et al.*, 1990), GCMs are less successful in reproducing the correct position of the storm tracks and of persistent anomalies. The storm tracks are shifted southwards in most simulations, especially in the European eastern parts where their northwest tilt is not captured (Chen and van den Dool, 1995; Déqué and Piedelievre, 1995; Murphy, 1995). Most regions of preferred occurrence of persistent anomalies are located correctly in the models, although the GCM-produced anomalies are less frequent and tend to be more persistent (Bates and Meehl, 1986; Blackmon *et al.*, 1984, Chen and van den Dool, 1995).

The large-scale circulation of the atmosphere in the extra-tropical regions can be described by the alternation of circulation types (CTs, henceforth), also known as weather regimes. These weather or climate, regimes are important factors in determining climate at various locations around the world and they can have a large impact on day-to-day variability (e.g. Plaut and Simmonet, 2001; Trigo *et al.*, 2004; Yiou and Nogaj, 2004). GCMs have been found to simulate hemispheric climate regimes quite similar to those found in observations (Robertson, 2001; Achatz and Opsteegh, 2003; Selten and Branstator, 2004). Simulated regional climate regimes over the North Atlantic strongly similar to the observed regimes were reported by Cassou *et al.*, (2004). Since the Third Assessment Report (TAR) of the IPCC, agreement between different studies has improved regarding the number and structure of both hemispheric and sectoral atmospheric regimes, but the statistical significance of the regimes has been discussed and remains an unresolved issue (e.g. Stephenson *et al.*, 2004; Molteni *et al.*, 2006).

Changes in the properties of the CTs are an important topic for the characterization of the variability of both observed climate and climate simulations. For instance, the identification of CTs associated with climate extreme events is expected to become increasingly important to determine the possible changes of climate extremes induced by the enhanced greenhouse effect (Sánchez Gómez and Terray, 2005). In this preliminary study we will focus on the main characteristics of the CTs and how their features would change under perturbed climate conditions. The latter could be important from a climate impact perspective.

CTs have been usually characterized by different subjective and objective classification methods. The subjective methods (Lamb, 1950) have been based on visual interpretation of the surface synoptic maps and show serious drawbacks, like the dependence of the assignment of a map to a particular pattern. In contrast, objective methods try to classify a set of maps using statistical techniques. Huth (1996) distinguished among four types of objective methods using correlations (Lund, 1963), sums of squares (Kirchhofer, 1973) as cost function, cluster analysis (Key and Crane, 1986; Kidson, 1994) and finally analysis based on eigentechniques (Richman, 1986). He found, in agreement with Jiang *et al.* (2006), that no method was indisputably superior.

Compagnucci and Salles (1997) used principal component analysis (PCA) to obtain CTs of daily July pressure fields over South America that were in good agreement with the types empirically identified by weather forecasters, enhancing the relevance of the human component. Richman (1986) employed different PCA-based techniques (in particular, PCA followed by either orthogonal or oblique rotation of the eigenvectors) to support the use of rotated solutions. Bartzokas and Metaxas (1996) also employed rotated PCA to avoid some drawbacks of the PCA. In spite of the benefits of rotation in PCA-based classifications, Compagnucci and Salles (1997) showed that sound classifications could also be obtained without rotation. Kyselý and Huth (2006) advocated, for the first time, the use of both objective and subjective classifications as complementary methods and, in fact, a growing body of opinion seems to support this point of view. In summary, experience suggests that it is up to the scientist to select, based mainly on experience and collaboration with synopticians, the most appropriate method according to the target of the study.

In the past, a large number of studies focused mainly on changes in frequencies of the Euro-Atlantic CTs: Slonosky *et al.* (2000) applying an EOF analysis revealed that the most important circulation regimes are the zonal and blocking/cyclonic flows in the eastern Atlantic and western Europe; Plaut and Simmonet (2001) found four 500-hPa regimes, Atlantic Ridge, Blocking, Greenland anticyclone, Greenwich Trough and Zonal with

interannual variability. Comparatively, few studies have focused on changes in the mean lifetime of the CTs. Recently, Kyselý and Domonkos (2006, KD henceforth) analyzed the Hess-Brezowsky (HB) classification (1952) of Grosswetterlagen over Europe since 1881 and noticed a sharp increase in the mean lifetime of the circulation patterns from the 1970s to the late 1980s for all seasons. Werner *et al.* (2000) were the first ones to identify the decade 1981-1990 as the onset of a shift in the Euro-Atlantic CTs on the basis of a change in mean lifetime of the west CT from the HB catalogue. Kyselý and Huth (2006) also found an increase around 1990 in the mean lifetime of atmospheric circulation in winter for all groups of their objectively defined CTs, although this increase was not as noticeable as for the HB CTs. This recent enhanced persistence of the atmospheric circulation may have also supported the more frequent occurrence of temperature and other climatic extremes in Europe recently and seems to be consistent with some climate change projections. It must also be taken into account that atmospheric blocking is a dynamical feature with major consequences for European climate (Doblas-Reyes *et al.*, 2002) and it is likely that the mean duration of certain CTs could be influenced by the extraordinary persistence of blocking events.

The studies concerned with simulations of the response of atmospheric circulation to increasing concentrations of greenhouse gases indicate that the enhanced greenhouse effect will lead to a slight northward shift of the midlatitude westerlies, while the change in their intensity is indeterminate. Both reduction and intensification are produced by different GCMs (Bates and Meehl, 1986; Mitchell *et al.*, 1990). There are also indications of decreasing intensity of meridional circulation and of reduction in the number of extratropical cyclones (Lambert, 1995; Carnell *et al.*, 1996). The predicted changes in circulation of smaller than global scales are less reliable and more model-dependent (Kidson and Watterson, 1995). Their unambiguous interpretation is difficult, especially when the strong response of a model appears in regions where its performance is poor.

Branderfelt and Kallen (2004) studying the response of the Southern Hemisphere circulation to an enhanced radiative greenhouse gas (GHG) forcing, have found that the spatial pattern of the leading mode of variability, the so-called Pacific-South American mode (Mo and Ghil, 1987) changed in response to the enhanced GHG forcing in a transient integration with a coupled global climate model (CGCM). This change is associated with changes in the propagation conditions for barotropic Rossby waves. Nevertheless, Branderfelt (2006), in the similar study for the Northern Hemisphere, found that the spatial patterns change in response to the enhanced forcing but the propagation conditions are unchanged.

The aim of this paper is twofold. Firstly, to provide an objective synoptic climatic classification of wintertime mid-tropospheric atmospheric circulation over the Euro-Atlantic domain, focusing on the estimates of frequency, mean lifetime, persistence and transitions using re-analysis data and simulations of present climate. As a second objective, the paper analyses the CTs obtained for perturbed climate simulations (2071-2100) under IPCC SRES A2 scenario. The text is organized as follows. The description of the datasets can be found in Section 2, the analysis of mean and standard deviation patterns in Section 3. The methodology is presented in Section 4. In Section 5 the Z500 CTs are analyzed in terms of their spatial structure (position and intensity of ridges and troughs) and temporal structure (frequency of occurrence and persistence). Special emphasis has been put on the analysis of persistence, which can be expressed in terms of the mean duration of events, defining an event as an uninterrupted sequence of days classified with one type, preceded and succeeded by days classified with another type. Sections 6 and 7 focus on trends and transitions of CTs respectively. Conclusions are summarized in Section 8. Annex I contains the figures and Annex II the tables.

2. DESCRIPTION OF DATASETS

Gridded (on a 2.5º x 2.5º degree latitude-longitude regular grid) daily 500-hPa geopotential height from the following datasets have been used:

a) Re-analysis produced at the European Centre for Medium-Range Weather Forecasts (**ERA40** henceforth; UPPALA *et al.*, 2005).

b) A simulation made with the second version of the Canadian Centre for Climate Modelling and Analysis (CCCma) Coupled Global Climate Model (**CGCM2** henceforth), which is based on the earlier CGCM1 but with some improvements aimed at addressing shortcomings identified in the first version. A description of CGCM2 can be found in FLATO *et al.* (2000). The atmospheric component of the model is essentially AGCM2 described by MCFARLANE *et al.* (1992). It is a spectral model with triangular truncation at wave number 32 (yielding a surface grid resolution of roughly 3.7° x 3.7°) and 10 vertical levels.

c) A simulation of the ECHAM climate model has been developed from the ECMWF atmospheric model (therefore the first part of its name, EC) and a comprehensive parameterisation package developed in Hamburg (therefore the abbreviation HAM), which allows the model to be used for climate simulations. The model is a spectral model with 19 atmospheric layers and the results used here derive from experiments performed with spatial resolution T42, which approximates to about 2.8º longitude/latitude resolution (ROECKNER *et al.*, 1992; and ROECKNER *et al.*, 1996).

d) A run of the third version of the model developed at the Hadley Centre (**HADCM3** henceforth) and described by GORDON *et al.* (1999). The atmospheric component of the model has 19 levels with a horizontal resolution of 2.5 degrees of latitude by 3.75 degrees of longitude, which produces a global grid of 96 x 73 grid cells (comparable to a spectral resolution of T42).

Data from the following two periods have been considered:

1) For the present climate, 1961-1990 for ERA40, CGCM2 and ECHAM4; 1961-1989 for HADCM3.

2) For the climate projections: 2071-2100 for CGCM2 and ECHAM4, and 2071-2089 for HADCM3. The Intergovernamental Panel on Climate Change (IPCC) published a Special Report on Emissions Scenarios (SRES) in 2000. This report describes the new set of emission scenarios used in the Third Assessment Report. In this study the SRES A2 scenario has been considered. SRES A2 scenario describes a very heterogeneous world, economic development is primarily regionally oriented and per capita economic growth and technological change is more fragmented and slower than in other storylines. The A2 uses data from an ensemble of three 111-year simulations using the provisional IPCC SRES A2 GHG and aerosol forcing scenario.

The study has been carried out for the extended winter season December-to-March (DJFM), which shows the largest variability over the extra-tropical Northern Hemisphere. The spatial domain considered is the Euro-Atlantic region, which extends from 25ºN to 70ºN and from 45ºW to 50ºE. All models have been interpolated to a common grid, (2.5º x 2.5º) of 741 grid points (39 in longitude and 19 in latitude). In the following, each winter is referred to with the year of the month of January included in the season.

3. MEAN AND STANDARD DEVIATION PATTERNS

Before proceeding to a detailed comparison between the simulated and the observed circulation (depicted in the re-analysis) results, it is useful to get an overall description of the 500 hPa mean and standard deviation (STD, henceforth) patterns (see Figures 1 and 2). In general, the control run simulated mean shows a very good agreement with respect to the re-analysis, whereas the simulated standard deviation tends to underestimate mainly in the northern area. The HADCM3 is the only one model which reproduces quite well the north Atlantic maximum of the re-analysis.

For the period 1961-1990, and taking the isoline of 5 760 m as reference, the mean pattern of CGCM2 shifts to southern latitudes the isoline of 5 760 m, meanwhile the STD pattern considerably underestimates the variability in northern areas. In ECHAM4 the 5 760 m isoline is shifted northwards and does not present the maximum of variability over Great Britain. The HADCM3 model is remarkably good at reproducing especially well the North Atlantic circulation features.

For the period 2071-2100, all the simulations shift northwards the 5 760 m isoline showing a more zonal behaviour which persists the variability underestimation with respect to the re-analysis. This underestimation of the variance might be attributed to some deficiencies in the treatment of physical processes in the GCMs, as mentioned by CHEN and VAN DEN DOOL (1995), it is a well-known deficiency of most GCM simulations.

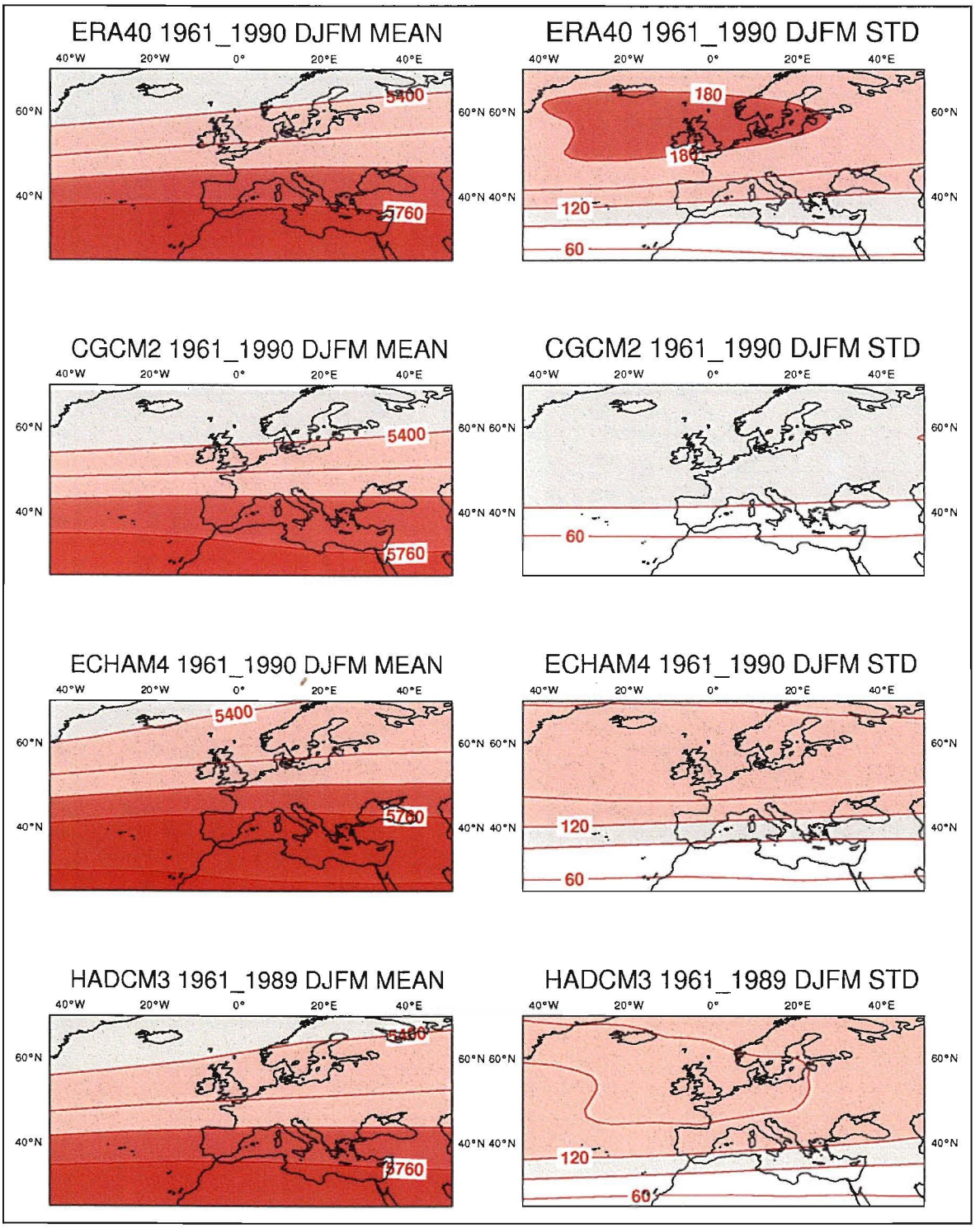

Figure 1. 500 hPa mean (left) and interannual standard deviation (right) for ERA40, CGCM2, ECHAM4 and HADCM3. Contours in metres.

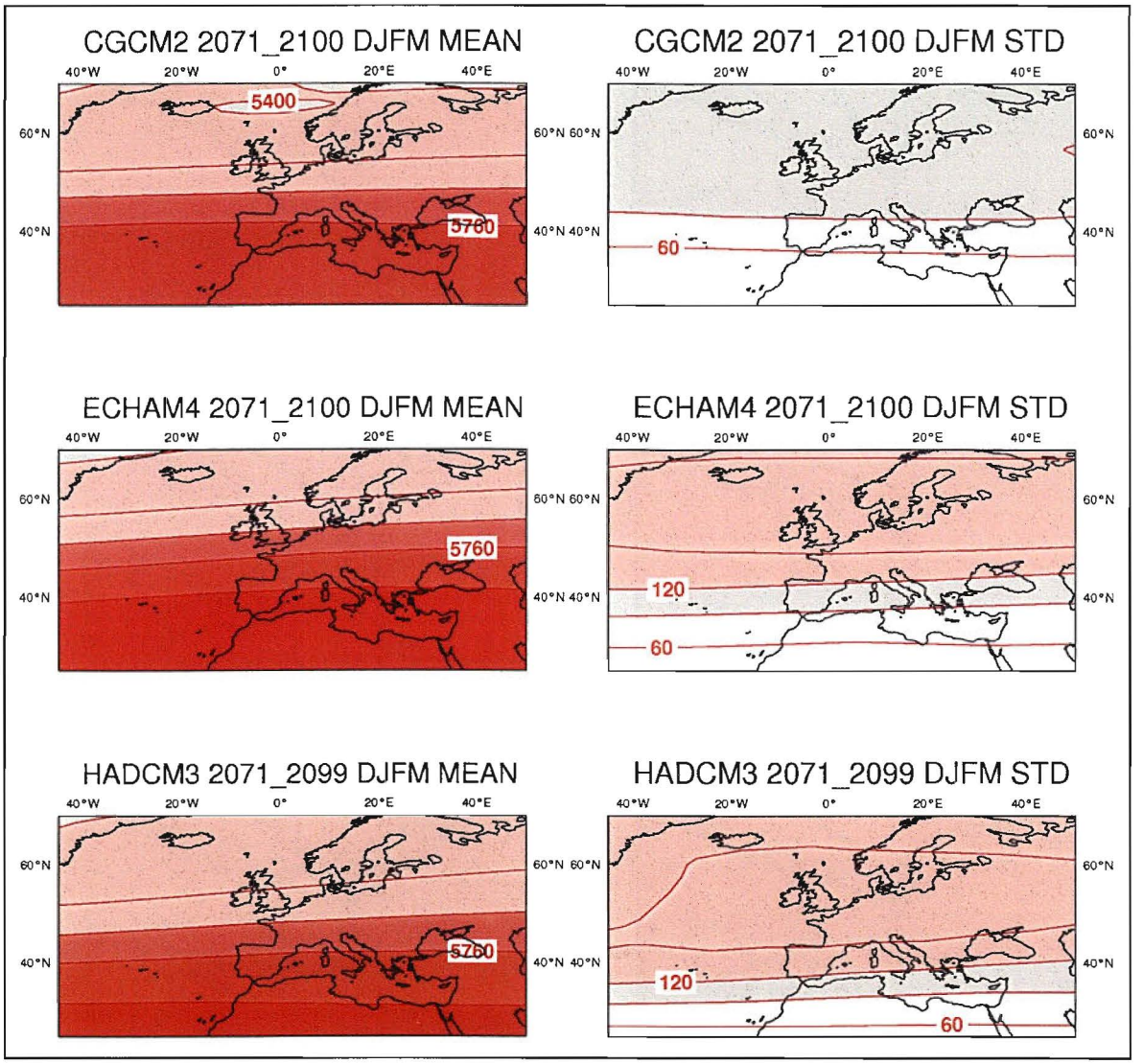

Figure 2. 500 hPa mean (left) and interannual standard deviation (right) for CGCM2, ECHAM4 and HADCM3. Contours in metres.

4. METHODOLOGY

The classification starts with a PCA, i.e. $\mathbf{Z} = \mathbf{F}\mathbf{A}^T$, where $\mathbf{Z}$ is the input data matrix ($N \times n$), $\mathbf{F}$ is the principal component (PC) score matrix ($N \times n$) and $\mathbf{A}$ is the loading matrix ($n \times n$), N being the number of observations and n the number of variables. The loadings, or empirical orthogonal functions (EOFs), are eigenvectors of a similarity matrix (covariance or correlation) $\mathbf{S} = (N-1)^{-1}\mathbf{Z}^T\mathbf{Z}$, scaled by the square root of the corresponding eigenvalues. The eigenvalues are the variance explained by each PC. Typically, many of the n dimensions of $\mathbf{A}$ represent mostly noise and are discarded based on some eigenvalue selection rules. The retained r eigenvectors produce a reduced matrix so $\mathbf{F}'$ ($N \times r$) while $\mathbf{A}$ becomes $\mathbf{A}'$ ($n \times r$) (RICHMAN, 1986; 1999).

The input data matrix $\mathbf{Z}$ can be specified in several ways, depending on which magnitudes are treated as variables and observations. Two possibilities are commonly used for a meteorological field; either the grid point values are referred to as variables and the time steps as observations, which is known as S-mode; or the time steps as variables and the grid points as observations in the so-called T-mode. While the S-mode isolates groups of grid points varying similarly in time, the T-mode isolates groups of time steps with similar spatial patterns. In this study we have applied the T-mode to obtain the CTs. We constructed $\mathbf{Z}$ from the winter unfiltered Z500 daily anomalies and carried out the PCA using a covariance matrix.

A shortcoming of the PCA is that the eigenvectors are mathematical constructions constrained by their mutual orthogonality and the maximization of variance over the entire analysis domain so that no link to physical entities is guaranteed. The use of PCA can force the analysis to merge or blend patterns that would be otherwise independent (RICHMAN, 1986). An alternative to reduce the effect of this drawback consists in rotating the empirical orthogonal functions and the corresponding PCs. The varimax orthogonal rotation (RICHMAN, 1986), which is the most widely used rotation technique with statistically stable patterns (CHENG and DUNKERTON, 1995), has been used. Following VON STORCH and ZWIERS (1999), the PCs were previously renormalized to have unit variance to keep them uncorrelated after rotation. The classification was carried out for both rotated and unrotated solutions, obtaining very similar CTs in both cases.

To determine the number r of PCs, a log-eigenvalue versus PC number (LEV) diagram was used (Figure 3). This diagram shows the log-eigenvalues for each PC in decreasing order. The number r is chosen as the number of log-eigenvalues which lie above the leftward extrapolation of the straight-line portion on its right hand side (WILKS, 2006). Figure 3 suggests a cut at the fourth eigenvalue. This choice is not unambiguous, so the impact of r have been studied examining the CTs obtained for different values of r. Tests were carried out with r ranging from 4 to 9. It can be concluded that the eight CTs obtained for $r = 4$ are very similar to the first eight CTs obtained for all the other values of r.

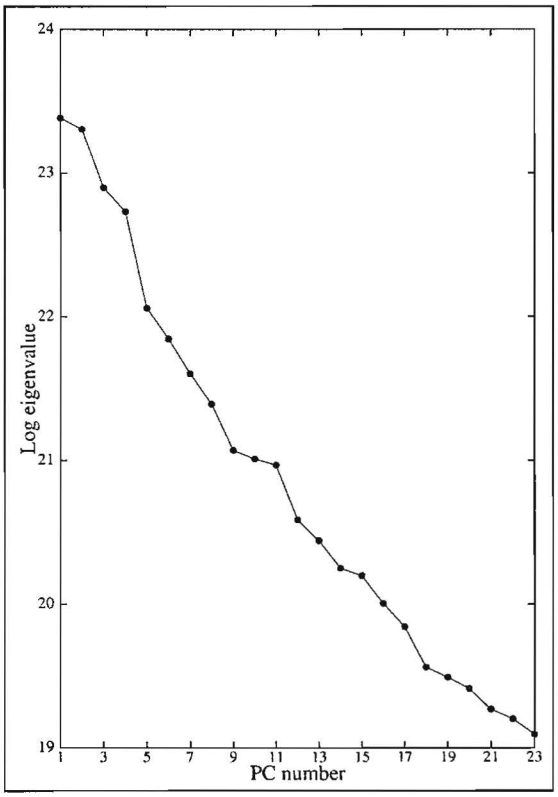

Figure 3. Log-eigenvalue versus principal component rank of the principal component analysis of the ERA40 500 hPa geopotential height dataset.

	1961-1990	2071-2100
ERA40	65.5	
CGCM2	66.4	66.4
ECHAM4	65.9	67.3
HADCM3	63.3	62.8

Table 1. Percentage of variance explained by the four leading rotated PCs considered.

The cumulative percentage of variance explained by the four leading rotated PCs is shown in Table 1. This table shows that except for HADCM3 all simulations overestimate the percentage of variance.

As the loadings may be either positive or negative, twice as many CTs as PCs can be obtained. In the case dealt with here, eight CTs are provided by the four rotated PCs. We have considered the CTs as the composites of the maps that are assigned to each CT.

The T-mode PCA approach results in score patterns describing frequently occurring maps. The loadings indicate how much a pattern explains a specific map, allowing the identification of time periods when the maps are similar in a statistical sense to specific patterns (Huth, 1997). The degree of similarity of a circulation pattern to a CT is expressed by the corresponding loading, the higher the loading (in an absolute sense) the greater the similarity. Therefore, each day's pattern is classified according to its highest loading (in the absolute sense).

5. CIRCULATION TYPES

5.1. 1961-1990

In this section CTs are analyzed taken into account frequency of occurrence, mean persistence and characteristics of duration of events.

The corresponding CTs composites for ERA40 are depicted in Figure 4 and a brief description of them can be found in Table a. There are common features of this classification with other classifications performed over the European region by different authors. Four of the CTs obtained closely resemble the four NCEP Z500 regimes identified by YIOU and NOGAJ (2004) using the clustering technique described in MICHELANGELI *et al.* (1995). Their regime "positive NAO" compares with ERA40_1, the "negative NAO" with the ERA40_6, the "Scandinavian blocking" with ERA40_3, and the "Atlantic ridge" with ERA40_4. However, YIOU and NOGAJ (2004) only considered four weather regimes, which makes impossible to match our eight CTs with their classification. Our results also compared well with the weather types identified by HUTH (1996, 2000) and with the HB-based objective classification published by JAMES (2007). For instance, the Cyclonic Westerly, Cyclonic Northerly, Icelandic High and Anticyclonic North Westerly are similar to the CTs ERA40_8, ERA40_4, ERA40_6, and ERA40_3, respectively.

With respect to the frequencies of occurrence, the maximum frequency corresponds to 15.29% (ERA40_1) and the minimum to 11.21% (ERA40_8) (see Table 2 in Annex II). The range of variation of the mean persistence varies between 2.44 days of ERA40_5 and the 3.88 days of ERA40_6 (see Table 3 in Annex II). As it can be observed, the most frequent type is not the most persistent type although it is ranked in the second position. Comparing with the CTs composites (see Figure 4), it seems that the less frequent types are connected with tilted ridges (NE-SW) approaching Iberia whereas the most frequent types are linked to ridges over the British Isles and Iceland.

Analysing Table 4, in Annex II, the mean duration is 3.16 days, the percentage of time spent in the events lasting four or more days is 62.34%, and the number of 1-day events is 399. Looking at Figure 8, in Annex I.1, events equal or longer than 15 days are registered, being the longest event of 17 days of duration (ERA40_6 and ERA40_7).

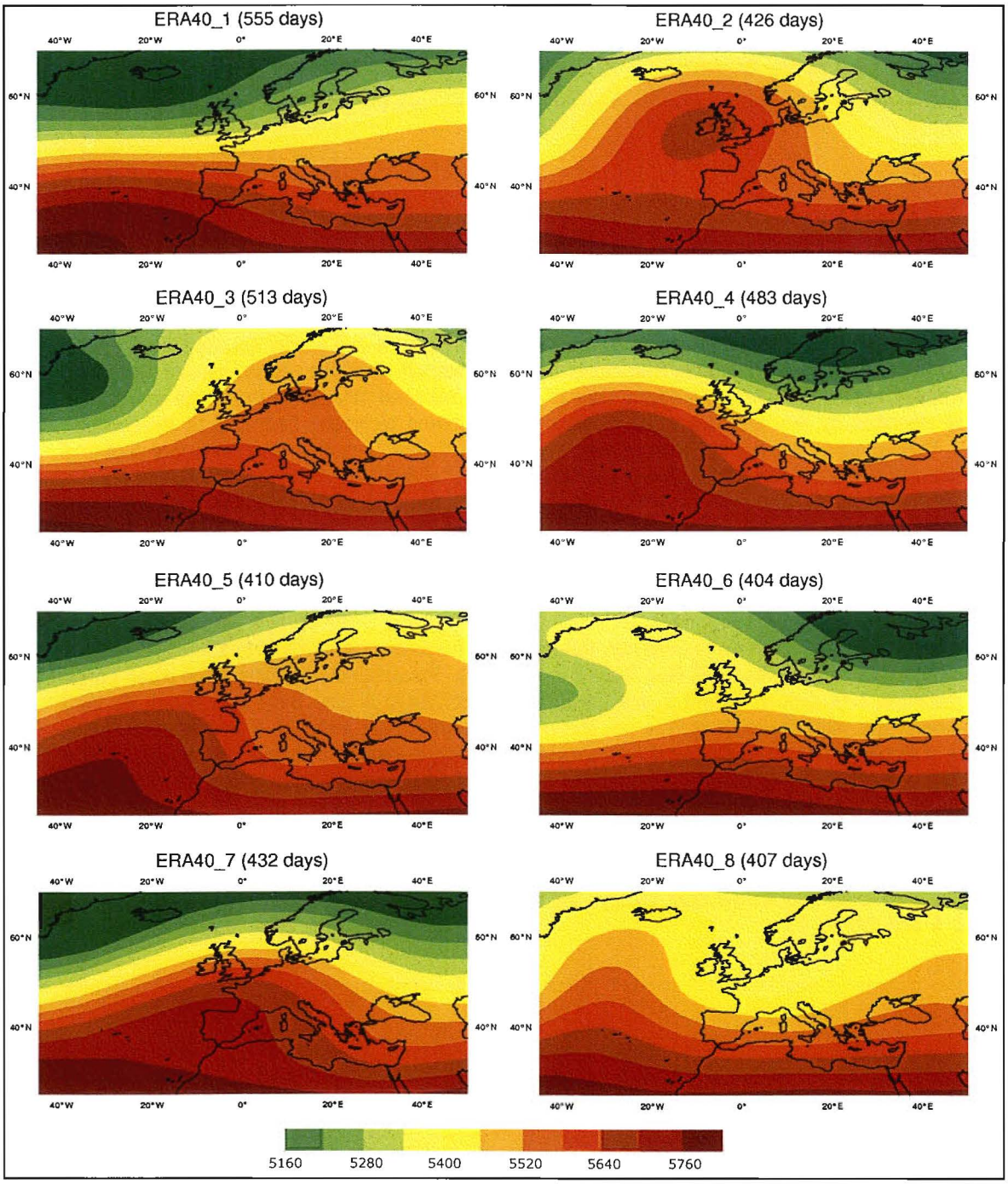

Figure 4. Circulation Types for the classification of the ERA40 500 hPa geopotential height over the period DJFM 1961-1990. Contour interval 60 mgp.

CTs (days)	Description
ERA40_1 (555)	Zonal flow
ERA40_2 (426)	Euro-Atlantic blocking with centre over British Isles
ERA40_3 (513)	Scandinavian blocking
ERA40_4 (483)	Atlantic ridge as an extension of the Azores anticyclone
ERA40_5 (410)	Ridge tilted from the southeast Atlantic to the central Europe
ERA40_6 (404)	Ridge over the British Isles and Iceland
ERA40_7 (432)	Ridge with axis from IP to Scandinavia
ERA40_8 (407)	Atlantic ridge with axis south of Iceland

Table a. Description of the ERA40 CTs. In parenthesis the total number of days

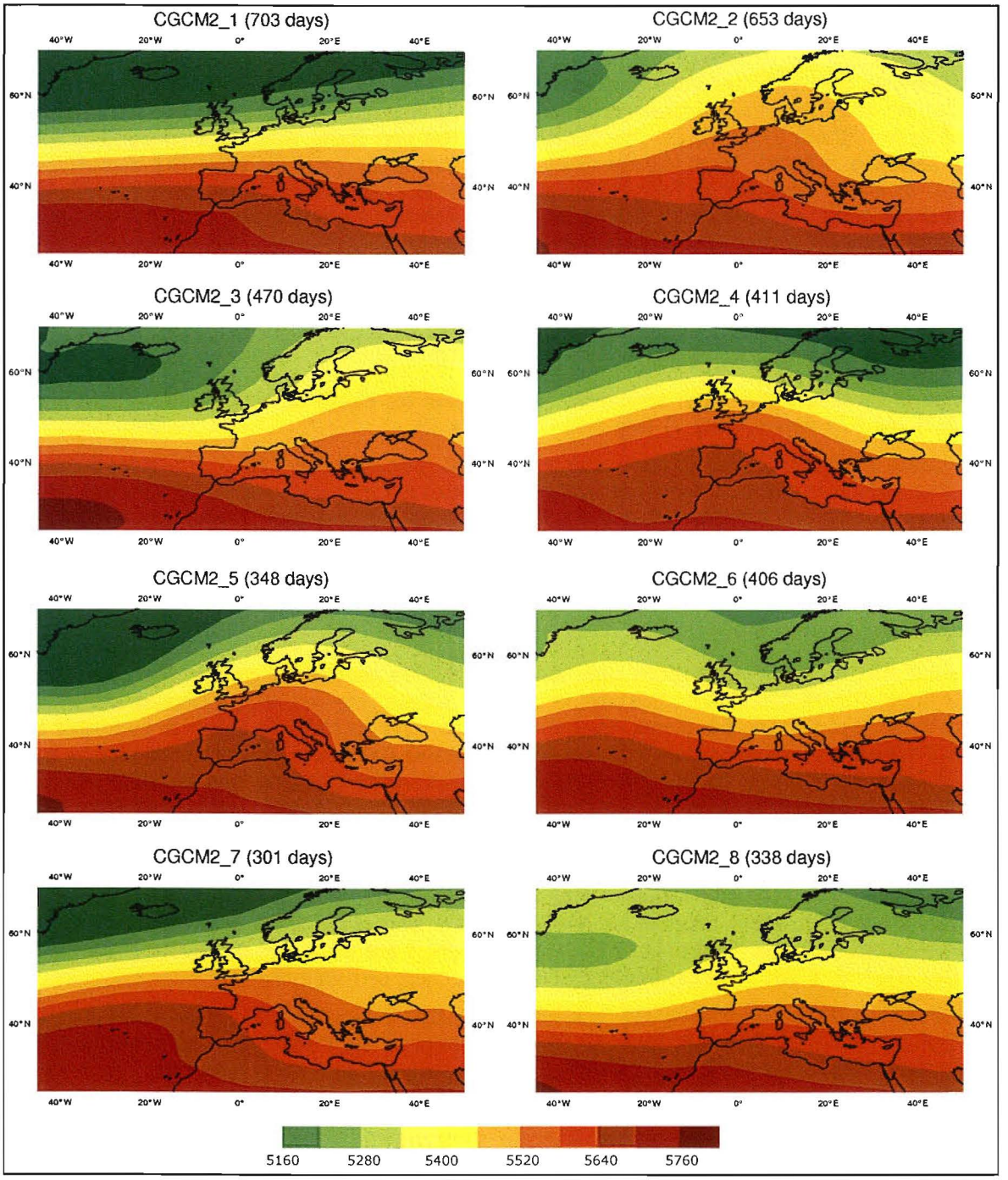

Figure 5. Circulation Types for the classification of the CGCM2 500 hPa geopotential height over the period DJFM 1961-1990. Contour interval 60 mgp.

CTs (days)	Description
CGCM2_1 (703)	Strong zonal flow
CGCM2_2 (653)	Scandinavian blocking
CGCM2_3 (470)	Zonal flow over the Atlantic and a ridge eastern Mediterranean
CGCM2_4 (411)	Ridge centred over British Isles
CGCM2_5 (348)	Ridge tilted from Canary Islands to Denmark
CGCM2_6 (406)	NW flow over IP, diffluence over eastern Mediterranean
CGCM2_7 (301)	Ridge tilted from the southeast Atlantic to the central Europe
CGCM2_8 (338)	Zonal flow south of British Isles

Table b. Description of the CGCM2 CTs for 1961-1990. In parenthesis the total number of days.

The corresponding CTs composites for CGCM2 (1961-1990) are depicted in Figure 5 and a brief description of them can be found in Table b.

As a general rule, the CGCM2 circulation types as compared to ERA40 (Figure 4) tend to exhibit more zonality, the ridges and troughs are much weaker. Euro-Atlantic blocking type (ERA40_2) and Atlantic ridge with axis south of Iceland (ERA40_8) are absent. The CGCM2_6, NW flow over Iberia, does not show similarity with the CTs presented in ERA40. These features might provide some evidence of the weakening of meridional circulation as it was also noted by Huth (1996) with the UKMO model and might be connected with the features shown in the mean and standard deviation patterns, where the corresponding to CGCM2 simulation shows more zonality.

CGCM2 CTs relative frequency of occurrence shows more differences among the types comparing with ERA40, oscillating between 19.37% (CGCM2_1) and 8.29% (CGCM2_7) (see Table 2 in Annex II). The less frequent type is connected with tilted ridges (NE-SW) approaching Iberia, as observed in ERA40, whereas the most frequent types is linked to zonal flow.

The range of variation of the mean persistence is larger than for ERA40 oscillating between 5.14 days (CGCM2_2) and 2.37 days (CGCM2_7) (see Table 3 in Annex II).

The circulation in the CGCM2 model is more persistent than the re-analysis (see Table 3). The mean duration is 3.61 days and the percentage of time spent in the events equal or longer than 4 days is 68.43% (see Table 4 in Annex II). It is worth mentioning that this is the most persistent simulation: 7 events longer than 18 days, being the longest event of 33 days of duration (CGCM2_1, see Figure 9 in Annex I.1). These features agree satisfactorily with the fact that CGCM2 has a smaller number of 1-day events.

The corresponding CTs composites for ECHAM4 (1961-1990) are depicted in Figure 6 and a brief description of them can be found in Table c.

As a general rule, the ECHAM4 circulation types show more 500 hPa geopotential gradient when comparing with ERA40 and with the CGCM2 circulation types respectively. Although the Euro-Atlantic blocking with centre over the British Isles (ERA40_2) is absent, there is a circulation type (ECHAM4_8) which can be treated as a blocking-ridge, and the Atlantic ridge with axis south of Iceland (ECHAM4_5) is much stronger than the corresponding ERA40_8 circulation type. Regarding the CGCM2 circulation types, the type connected with NW flow over Iberia is also present (ECHAM4_7) but reinforced. More number of Atlantic ridges are observed than in ERA40.

The range of variation of the relative frequencies of occurrence (see Table 2 in Annex II) is smaller than in the CGCM2 simulation, oscillating between 15.42% (ECHAM4_1) and 10.28% (ECHAM4_7). The higher frequencies are linked to strong ridges in the Atlantic, south or west of the British Isles. The range of the mean persistence days varies between the 2.92 days of ECHAM4_8 and the 4 days of ECHAM4_6 (see Table 3 in Annex II). As in ERA40 the most frequent CT is not the most persistent one.

Table 4 shows that the number of 1-day events is 306, smaller than the corresponding to ERA40 and a mean duration of 3.36 days (see Table 4 in Annex II). ECHAM4 simulation has 6 events equal or longer than 15 days, being the longest one of 22 days (ECHAM4_6) as it is seen in Figure 10, in Annex I.1.

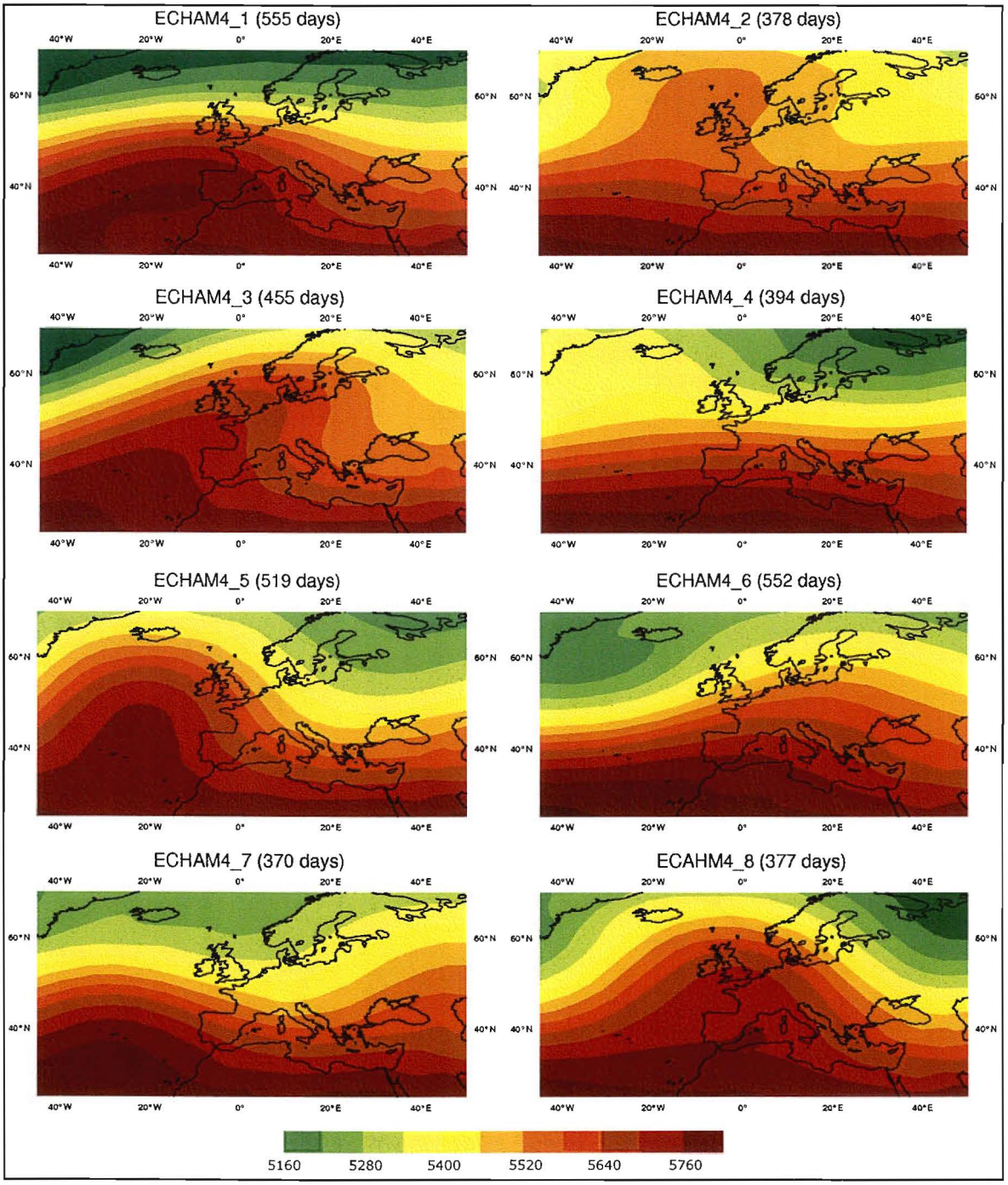

Figure 6. Circulation Types for the classification of the ECHAM4 500 hPa geopotential height over the period DJFM 1961-1990. Contour interval 60 mgp.

CTs (days)	Description
ECHAM4_1 (555)	Strong Atlantic ridge centred southern British Isles
ECHAM4_2 (378)	Atlantic ridge centred between Iceland and the British Isles
ECHAM4_3 (455)	Ridge tilted from the southeast Atlantic to Bothnian Gulf
ECHAM4_4 (394)	Strong zonal flow south of the British Isles. Trough over Finland
ECHAM4_5 (519)	Strong Atlantic ridge as an extension of the Azores anticyclone
ECHAM4_6 (552)	Ridge over central and eastern Europe
ECHAM4_7 (370)	Weak trough over Norwegian Sea. NW flow over IP
ECHAM4_8 (377)	Strong ridge centred over the British Isles

Table c. Description of the ECHAM4 CTs for 1961-1990. In parenthesis the total number of days.

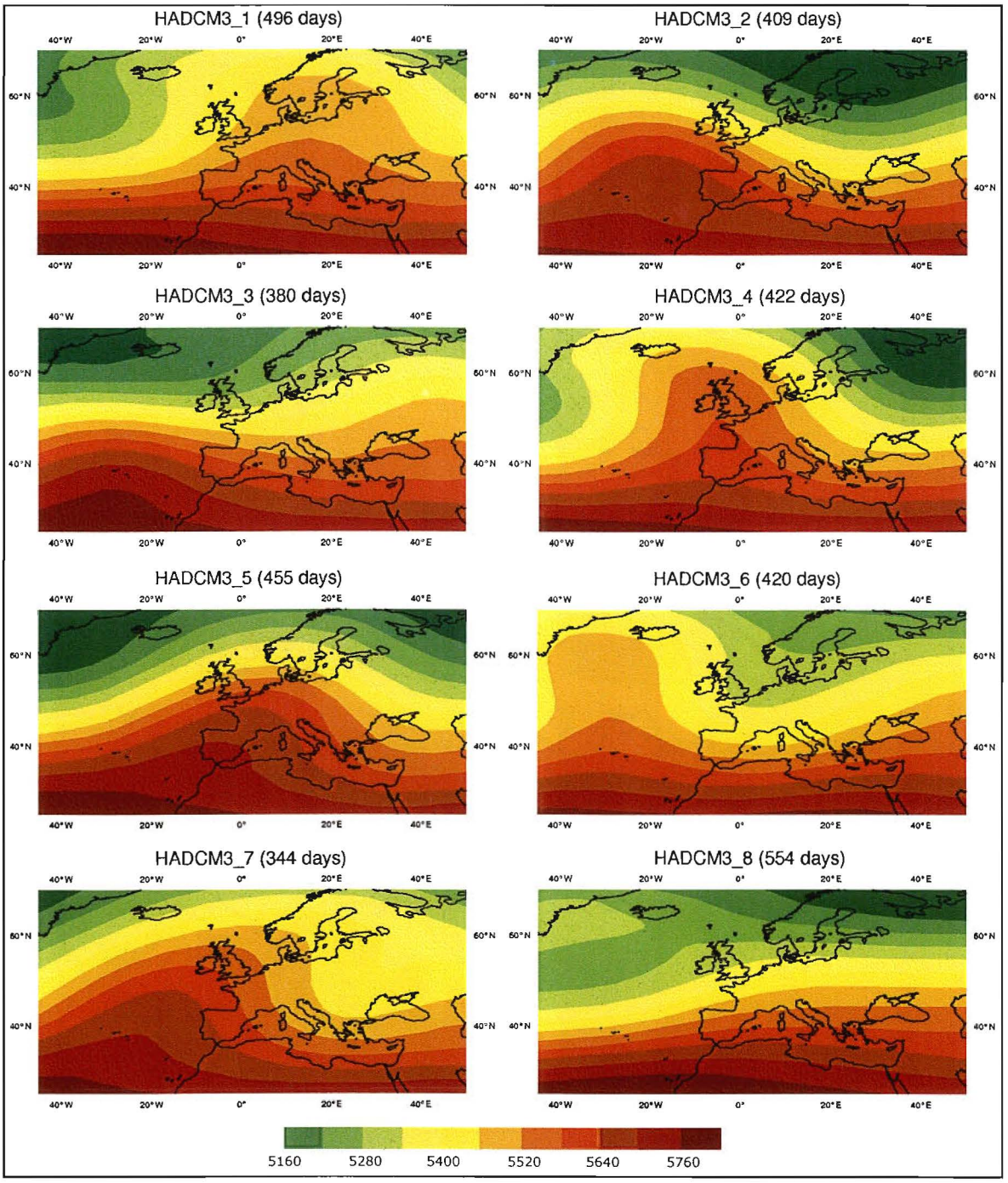

Figure 7. Circulation Types for the classification of the HADCM3 500 hPa geopotential height over the period DJFM 1961-1989. Contour interval 60 mgp.

CTs (days)	Description
HADCM3_1 (496)	Scandinavian blocking
HADCM3_2 (409)	Atlantic ridge as an extension of the Azores anticyclone
HADCM3_3 (380)	Zonal flow
HADCM3_4 (422)	Atlantic ridge centred over the British Isles
HADCM3_5 (455)	Ridge with axis from IP to Scandinavia
HADCM3_6 (420)	Atlantic ridge with axis west-southwest of Iceland
HADCM3_7 (344)	Ridge tilted from the southeast Atlantic to the central Europe
HADCM3_8 (554)	Ridge over the British Isles and Iceland

Table d. Description of the HADCM3 CTs for 1961-1989. In parenthesis the total number of days.

The corresponding CTs composites for HADCM3 (1961-1989) are depicted in Figure 7 and a brief description of them can be found in Table d.

HADCM3 CTs shows more similitude with the ERA40 ones than the other two climate simulations.

The range of variation of the relative frequencies of occurrence of the HADCM3 varies from 15.92% (HADCM3_8) to 9.89% (HADCM3_7) (see Table 2 in Annex II). The less frequent situation is linked to tilted ridges near Iberia and the most frequent is related with zonal flow as it occurs in ERA40 and the other simulations. A coincidence is detected between the (most/less) frequent type and the (most/less) persistent type. The range of the mean persistence varies between the 2.51 days of HADCM3_7 and the 3.30 days of HADCM3_8 (see Table 3 in Annex II).

Table 4 shows that the number of 1-day events (515 days), overestimates in more than the 100 days the corresponding of ERA40, and the mean duration, 2.85 days which is the least one (we have to bear in mind that HADCM3 has only 29 winters). HADCM3 simulation has 13 events equal or longer than 15 days, being the longest event of 34 days of duration (HADCM3_5), this latter feature reminds of the corresponding CGCM2 characteristic (see Figure 11 in Annex I.1).

5.2. 2071-2100 (SRES A2)

To evaluate the possible impact of emission scenarios upon circulation we have analyzed the Circulation Types features of the above mentioned simulations for the perturbed climate over the period (2071-2100) under SRES A2 in order to study more precisely the behaviour in the last part of the century.

The corresponding CTs composites for CGCM2 (2071-2100) are depicted in Figure 12 and a brief description of them can be found in Table e.

The circulation types exhibit more zonality compared with the control (CGCM2 1961-1990). When analysing the relative frequencies of occurrence the range of variation of the frequencies is larger than for 1961-1990, oscillating between 21.87% (CGCM2_A2_1) and 7.43% (CGCM2_A2_8) (see Table 5 in Annex II). The mean persistence time ranges from 4.81 days (CGCM2_A2_2) and 2.09 days (CGCM2_A2_8) (see Table 6 in Annex II).

A slight decrease of the mean duration, 3.33 days, versus the 3.61 days of the CGCM2 1961-1990 is noticed. Accordingly, a great number of 1-day events and a small percentage of time spent, in the events equal or longer than 4 days, it is detected (see Table 7 in Annex II).

There are 20 events equal or longer than 15 days, being the largest event of 27 days (CGCM2_A2_1) (see Figure 15 in Annex I.2).

The corresponding CTs composites for ECHAM4 (2071-2100) are depicted in Figure 13 and a brief description of them can be found in Table f.

In the ECHAM4_A2_2071-2100, the range of variation of the relative frequencies of occurrence is smaller than in the CGCM2_A2_2071_2100, oscillating between 16.61% (ECHAM4_A2_1) and 7.92% (ECHAM4_A2_8) (see Table 5 in Annex II), this range of variation is smaller than the corresponding to ECHAM4_1961_1990.

The mean persistence ranges from 1.83 days (ECHAM4_A2_7) to 3.96 days (ECHAM4_A2_2), (see Table 6 in Annex II).

The response of the atmospheric circulation when considering the SRES A2 scenario is also manifested in a decrease of the mean duration, 2.75 days, versus the 3.36 days for ECHAM4_1961_1990. Accordingly, a large number of 1-day events and a small percentage of time spent, in the events equal or longer than 4 days, it is detected (see Table 7 in Annex II). Finally, as far as the behaviour of the longest events is concerned, ECHAM4_A2_2071_2100 presents 5 events equal or longer than 15 days, being the longest one of 19 days duration (ECHAM4_A2_6) (see Figure 16 in Annex I.2).

The corresponding CTs composites for HADCM3 (2071-2099) are depicted in Figure 14 and a brief description of them can be found in Table g.

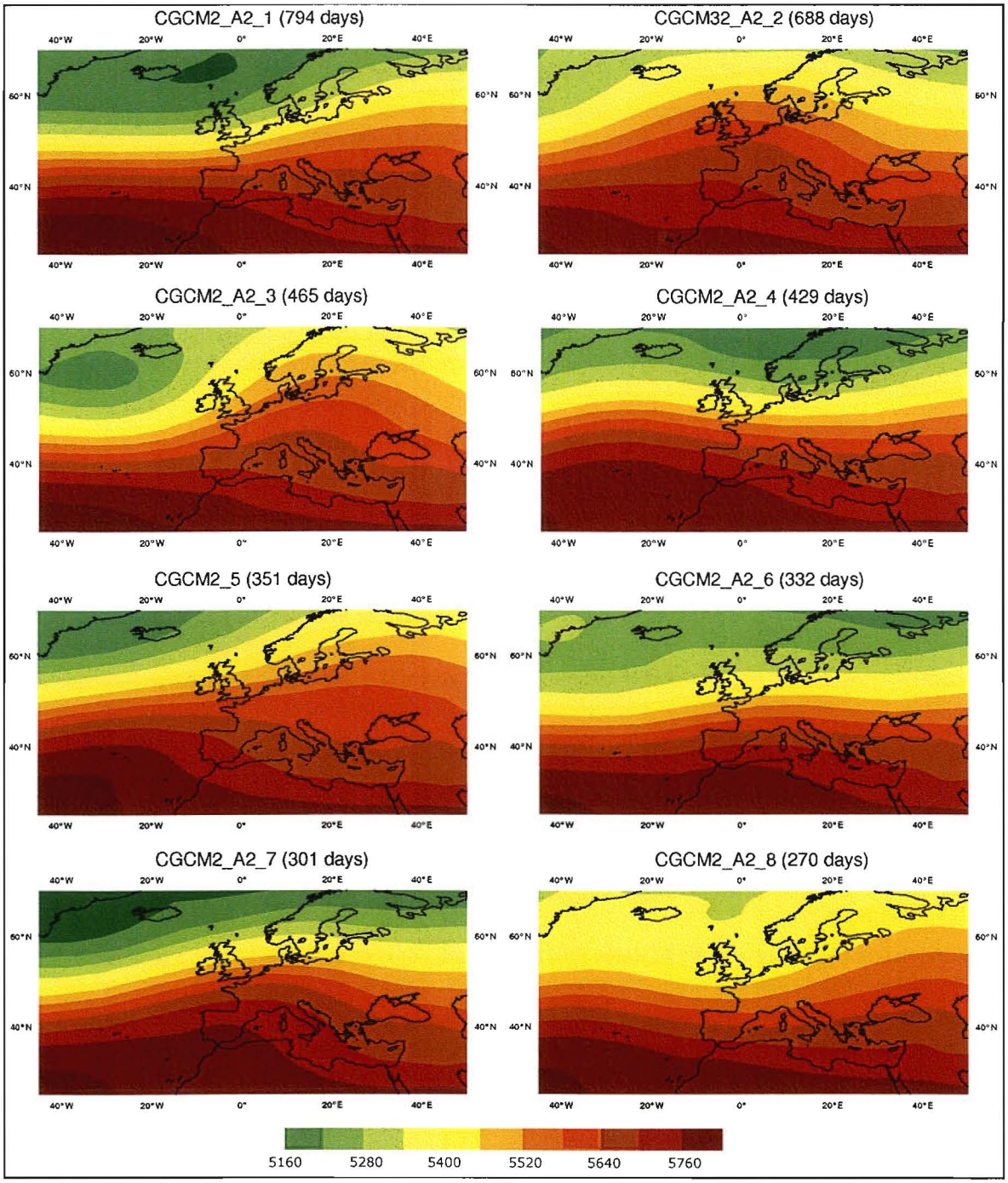

Figure 12. Circulation Types for the classification of the CGCM2 500 hPa geopotential height over the period DJFM 2071-2100. Contour interval 60 mgp.

CTs (days)	Description
CGCM2_A2_1 (794)	Strong zonal flow. Jet shifted northwards
CGCM2_A2_2 (688)	Ridge tilted from Bothnian Gulf to Lion Gulf
CGCM2_A2_3 (465)	Zonal flow over the IP and Med. Sea and anticyclonic flow over western Europe and Scandinavia
CGCM2_A2_4 (429)	Atlantic ridge southern part of the British Isles, weak trough over western Europe
CGCM2_A2_5 (351)	Ridge with axis from IP to Scandinavia
CGCM2_A2_6 (332)	Zonal flow south of France, weak trough between Iceland and Norway
CGCM2_A2_7 (301)	Anti-cyclonic flow over western and southern Europe
CGCM2_A2_8 (270)	NW flow over IP, ridge over eastern Europe

Table e. Description of the CGCM2 CTs for 2071-2100. In parenthesis the total number of days.

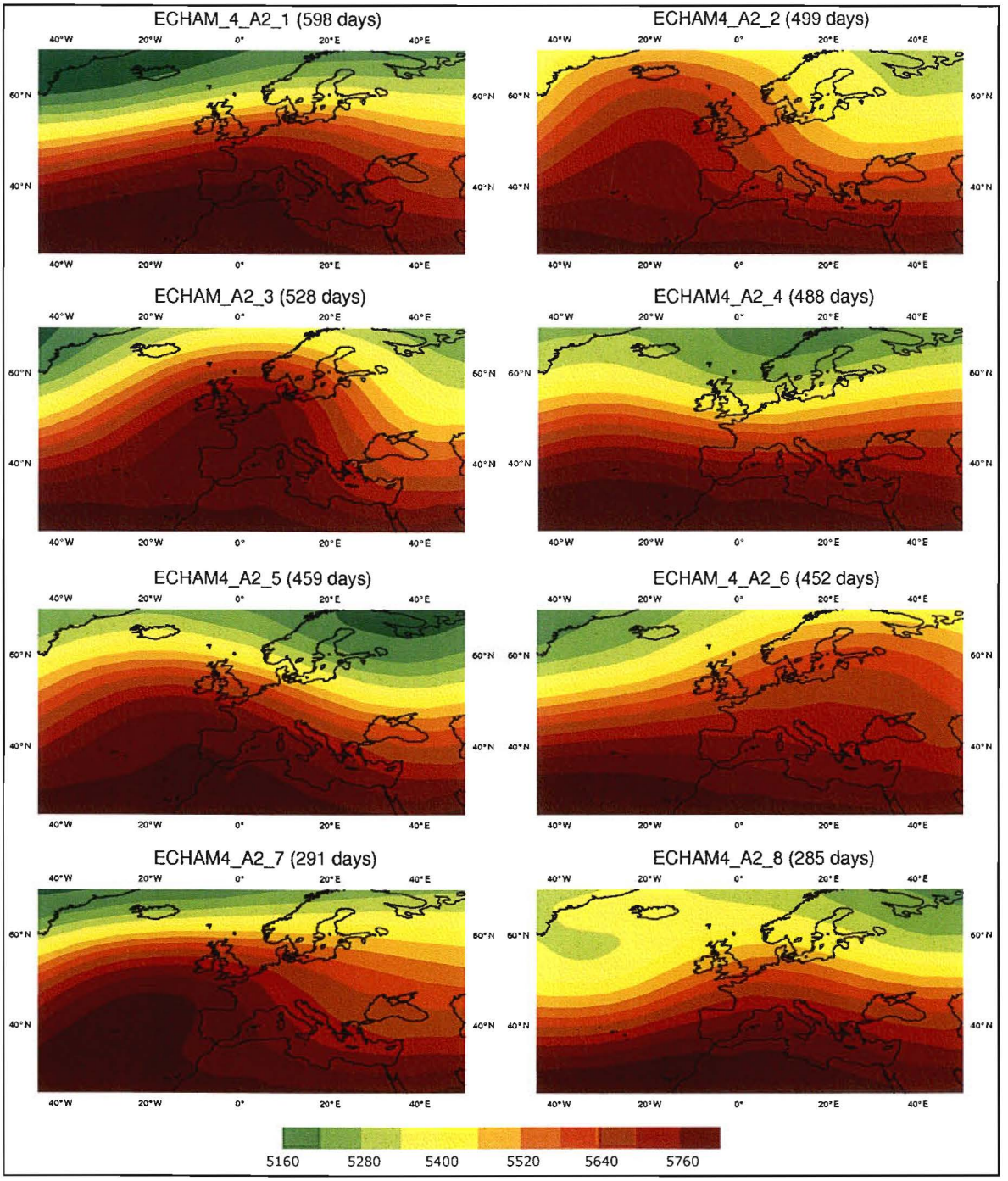

Figure 13. Circulation Types for the classification of the ECHAM4 500 hPa geopotential height over the period DJFM 2071-2100. Contour interval 60 mgp.

CTs (days)	Description
ECHAM4_A2_1 (598)	Ridge over southern Denmark
ECHAM4_A2_2 (499)	Atlantic ridge southern Iceland
ECHAM4_A2_3 (528)	Strong ridge from IP to southern Scandinavia
ECHAM4_A2_4 (488)	Zonal flow affecting mainly central and southern Europe
ECHAM4_A2_5 (459)	Strong Atlantic ridge western the British Isles
ECHAM4_A2_6 (452)	Tilted ridge from Bothnian Gulf to the Balkans
ECHAM4_A2_7 (291)	Tilted ridge southwestern British Isles and diffluence over Balkans
ECHAM4_A2_8 (285)	Ridge western Europe

Table f. Description of the ECHAM4 CTs for 2071-2100. In parenthesis the total number of days.

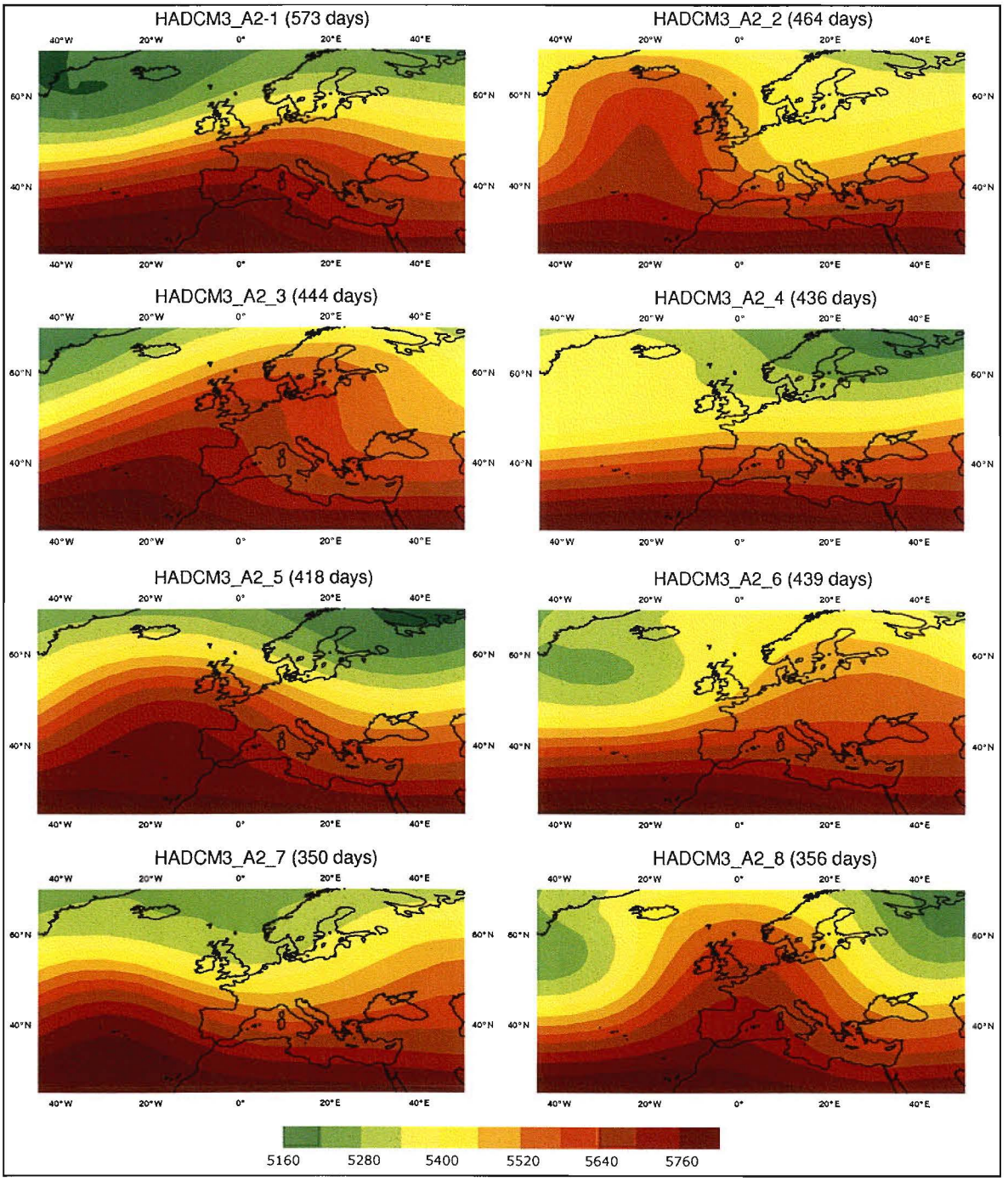

Figure 14. Circulation Types for the classification of the HADCM3 500 hPa geopotential height over the period DJFM 2071-2099. Contour interval 60 mgp.

CTs (days)	Description
HADCM3_A2_1 (573)	Ridge over southern Denmark
HADCM3_A2_2 (464)	Atlantic ridge southern Iceland
HADCM3_A2_3 (444)	Strong ridge from IP to southern Scandinavia
HADCM3_A2_4 (436)	Zonal flow affecting mainly central and southern Europe
HADCM3_A2_5 (418)	Strong Atlantic ridge western the British Isles
HADCM3_A2_6 (439)	Tilted ridge from Bothnian Gulf to the Balkans
HADCM3_A2_7 (350)	Tilted ridge southwestern British Isles and diffluence over Balkans
HADCM3_A2_8 (356)	Ridge western Europe

Table g. Description of the HADCM3 CTs for 2071-2099. In parenthesis the total number of days.

The range of variation of the relative frequencies of occurrence of the HADCM3_A2_2071_2099 varies from 16.46% (HADCM3_A2_1) and 10.06% (HADCM3_A2_7), Table 5 in Annex II. The most frequent CTs are related with strong ridges and zonal flows as it was in ERA40.

The range of the mean persistence varies between the 3.89 days of HADCM3_A2_4 and the 2.63 days of HADCM3_A2_7 (see Table 6 in Annex II). The mean duration is 3.40 days which is the largest one in of the three simulations considered.

The number of 1-day events is also the smallest, 308 days, (see Table 7 in Annex II), noticeably smaller than the corresponding to HADCM3_1961_1989 (515 days). 15 events equal or longer than 15 days are detected, being the longest event of 39 days of duration (HADCM3_A2_71_99_8), associated to a blocking-like ridge, a record in the datasets considered in this study, (see Figure 17 in Annex I.2).

6. TRENDS IN THE CIRCULATION TYPES FREQUENCY

6.1. 1961-1990

The time evolution of the CTs frequency for the period 1961-1990 is shown for ERA40 and for the three model simulations in Figures 18-21 in Annex I.3. The red line represents the linear trend.

As a general rule, the inter-annual variability of the CT frequency is high, with some CTs happening more than one third of the days in a winter, whereas other CTs do not happen at all. There is also some decadal variability.

For the ERA40 re-analyses (see Figure 18 in Annex I.3), there is an increase in the frequency of ERA40_7, a ridge with axis from the IP to Scandinavia, from the 1970s to the early 1990s in agreement with Casado *et al.* (2007), using the same re-analysis but with an extended period. There is a slight positive trend in ERA40_1 and a negative trend in ERA40_2, which might be statistical significant, connecting with a decrease in the frequency of the Euro-Atlantic blockings. Another negative trend is observed in the frequency of ERA40_8, related to what it is named by other authors, Greenland anticyclone.

For the CGCM2 simulation (see Figure 19 in Annex I.3), the most outstanding features concerns the strong positive trend in CGCM2_2, the Scandinavian blocking, especially in comparison with the same CT in ERA40 in which practically no trend or slightly positive trend. Negative trends affecting the frequency of CGCM2_4, a ridge centred over the British Isles and the CGCM2_1, strong zonal flow, have been also observed.

For the ECHAM4 simulation (see Figure 20 in Annex I.3), the trends in the frequency seem to be smoother than in the other simulations, excepting the positive trend in ECHAM4_5, strong Atlantic ridge as an extension of the Azores anticyclone and the negative trend affecting the frequency of ECHAM4_7 and ECHAM4_8 -strong ridge centered over the British Isles, in agreement with the CGCM2.

For the HADCM3 simulation (see Figure 21 in Annex I.3), there is an increase in the frequency of the HADCM3_5, a ridge with axis from the IP to Scandinavia as in ERA40. Slight positive trend concerns the frequency of the Scandinavian blocking (HADCM3_1). Negative trend affects the frequency of the HADCM3_2, Atlantic ridge linked to an extension of the Azores anticyclone but located westwards with respect to the analogous circulation type of ERA40. A weak negative trend is observed in the frequency of HADCM3_3, NW flow over the IP. The remaining CTs depict practically no trend.

6.2. 2071-2100 (SRES A2)

The time evolution of the CTs frequency for the SRES A2 scenario for the period 2071-2100 and for the three future climate simulations is shown in Figures 22-24 in Annex I.4. The red line represents the linear trend.

For the CGCM2 SRES A2 simulation (see Figure 22 in Annex I.4), the most noticeable feature is the positive trend in the frequency of the CGCM2_A2_7, a ridge with axis from Denmark to northwest Africa and a slight positive trend in the frequency of the CGCM2_A2_1, strong zonal flow. There is a strong negative trend observed in the frequency of the CGCM2_A2_8, NW flow affecting central and southern Europe.

For the ECHAM4 SRES A2 simulation (see Figure 23 in Annex I.4), the trends in the frequency seem to be smoother than in the other simulations, excepting the negative trends which concern the frequency of the ECHAM4_A2_2, Atlantic ridge southern Iceland, and the frequency of ECHAM4_A2_6, a tilted ridge from Bothnian Gulf to the Balkans. A weak positive positive trend is observed in the frequency of ECHAM4_A2_7, tilted ridge over the southwest of the British Isles and diffluence over Balkans and the frequency of ECHAM4_A2_1, a ridge over southern Denmark.

For the HADCM3 SRES A2 simulation (see Figure 24 in Annex I.4), the trends in the frequency of the CTs are quite similar to the ECHAM4 SRES A2. There is a positive increase in the frequency of the HADCM3_A2_3, a ridge with axis from the IP to Scandinavia. Slight positive trend concerns the frequency of the zonal flow affecting mainly central and southern Europe, HADCM3_A2_4. Negative trend is observed mainly in the frequency of HADCM3_A2_2, Atlantic ridge over southern Iceland. The remaining CTs depict scarcely no trend.

By way of summary, the inter-annual variation of the CT frequency is rather high, as it is for the 1961-1990 period. The results seem to be model-dependent, although there is agreement in the positive trend which affects the frequency of a ridge with axis from the IP to Scandinavia and to a lesser extent to some zonal-like flow.

7. TRANSITIONS BETWEEN CIRCULATION TYPES

7.1. 1961-1990

The development of a transition may be a process purely internal to the atmospheric dynamics connected to phase changes of intra-seasonal atmospheric waves as suggested by SÁNCHEZ GÓMEZ and TERRAY (2005). JAMES (2007) has recently pointed out that if any particular Grosswetterlagen is followed by a small number of specific types, a measure of medium-range predictability could be obtained. At present CTs are quite well known but understanding the processes associated with transitions between them, which are perhaps the most significant feature, is another matter entirely.

In this study, we have used the transitions as a tool to detect any particular and subtle differences between the CTs of the study.

The transitions between a specific CT and any of the other CTs are described for ERA40 and the three model simulations over the period 1961-1990 in Tables 8-11, in Annex II. The transitions are expressed (in percentage) as the ratio between the number of changes from a CT to another one to the total number of changes from that CT (re-entries into the same CT are excluded).

For the ERA40 re-analyses the transition matrix of ERA40 (see Table 8 in Annex II), 7 transitions are unlikely. These are mainly located in the diagonals adjacent to the main diagonal. Among these unlikely transitions, we outline the Euro-Atlantic blocking to zonal flow, Scandinavian blocking to an Atlantic ridge as an extension of the Azores anticyclone. For the remaining possible transitions (49) the most probable (30%) occur from the Scandinavian blocking (ERA40_3) to a ridge tilted from the South-East Atlantic to Central Europe (ERA40_5) and from a ridge with axis from the IP to Scandinavia (ERA40_7), which is linked to the positive phase of NAO, to the zonal flow (ERA40_1) or from the Atlantic ridge as an extension of the Azores anticyclone (ERA40_4) to ERA40_1.

For the CGCM2 simulation, the matrix of transitions (see Table 9 in Annex II) illustrates that 6 out of 56 possible transitions do not take place. They are located, as in ERA40, in the lines parallel to the main diagonal (for instance, Scandinavian blocking to strong zonal flow). The transitions most frequent are larger than those found for ERA40. The most probable transitions (32%) occur from a ridge tilted from the south-east Atlantic to Europe (CGCM2_7) to strong zonal flow (CGCM2_1) and from a ridge centred over the British Isles (CGCM2_4) to a ridge tilted from Canary Islands to Denmark (CGCM2_5).

For the ECHAM4 simulation, the matrix of transitions (see Table 10 in Annex II) reveals as in ERA40 and CGCM2 that 7 out of 56 possible transitions are unlikely. As said previously, these unlikely transitions tend to be located in the lines parallel to the main diagonal (for instance, strong Atlantic ridge as an extension of the Azores anticyclone to a ridge over central and eastern Europe; strong zonal flow south of the British Isles to a ridge tilted from the south-east Atlantic to Bothnian Gulf, connected to Scandinavian blocking). The most probable transition (31%) occurs from a ridge tilted from the south-east Atlantic to Bothnian Gulf (ECHAM4_3) to a strong Atlantic ridge centred southern British Isles (ECHAM4_1).

For the HADCM3 simulation, the matrix of transitions (see Table 11 in Annex II), contrarily to ERA40 and the other two model simulations, shows that the 56 possible transitions are likely. The less frequent transition (0.65%) takes place between a ridge with axis from the IP to Scandinavia (HADCM3_5) to a Atlantic ridge with axis west-southwest of Iceland. The most frequent transitions have a lesser frequency that in ERA40 and the simulations. The most probable transition (24%) occurs from a ridge with axis from IP to Scandinavia (HADCM3_5) to zonal flow (HADCM3_3).

7.2. 2071-2100 (SRES A2)

To understand global warming and its implication for climate in general, we need to understand the dynamics of atmospheric regimes and regime change (PALMER 1999).

The transitions between a specific CT and the other CTs are described for future climate simulations in Tables 12-14 in Annex II. As a general rule, it seems that there is a notorious increase in the frequency of some transitions comparing with the corresponding to the 1961-1990 period, and it is apparent that the number of unlikely transitions has diminished.

For the CGCM2 simulation, the transition matrix (see Table 12 in Annex II), there are 4 unlikely transitions of the possible 56. The most probable transitions (42%) occur from a ridge with axis from the IP to Scandinavia (CGCM2_A2_5) to strong zonal flow (CGCM2_A2_1).

For the ECHAM4 simulation, the transition matrix (see Table 13 in Annex II), only 4 out of the possible transitions are unlikely. The most probable transitions (41%) occur from Atlantic ridge southern Iceland (ECHAM4_A2_2) to a strong ridge from IP to southern Scandinavia (ECHAM4_A2_3) and from a ridge over southern Denmark (ECHAM4_A2_1) to zonal flow affecting mainly central and southern Europe (ECHAM4_A2_4).

For the HADCM3 simulation, the transition matrix (see Table 14 in Annex II), only 4 out of the possible transitions are unlikely. The most probable transitions (38%) occur between a ridge over the North-Sea, a kind of blocking (HADCM3_A2_8) to a strong ridge from the IP to Scandinavia (HADCM3_A2_3).

8. CONCLUSIONS

The Euro-Atlantic atmospheric circulation types resulting from an objective classification using the ERA40 re-analysis and three climate model simulations (CGCM2, ECHAM4 and HADCM3) have been examined for the extended winter period. The resulting circulation types have been applied: 1) to validate continental-scale circulation in control runs against re-analyses, and 2) to estimate changes in continental-scale circulation under SRES A2 scenario projections.

The classification algorithm is based on a T-mode PCA followed by a varimax rotation of the four leading PCs. This classification shows most of the mainly features presented in previous studies.

8.1. 1961-1990

As a general rule, in the period 1961-1990, the ECHAM4 circulation types have the biggest geopotential gradient compared with ERA40 and with the CGCM2 circulation types respectively. For instance, although the Euro-Atlantic blocking with centre over the British Isles is absent, there is a type which can be treated as a blocking-ridge. The HADCM3 circulation types share many characteristics in common with ERA40.

The behaviour of the relative frequencies of the CTs is rather similar in ERA40 and the three model simulations considered. In ERA40, the most frequent CT is the zonal flow (15%) while the less frequent CTs are the ridges over the Atlantic at different latitudes. In the CGCM2, more differences are detected among the types (19% vs 8%), being the less frequent CT linked to tilted ridges (NE-SW) approaching Iberia. In the ECHAM4, the range of variation is smaller than for CGCM2 (15% vs 10%), being the higher frequencies linked to strong ridges in the Atlantic, south or west of the British Isles. In the HADCM3 (15% vs 10%), the less frequent CT is linked to tilted ridges near Iberia and the most frequent is related with the zonal flow.

There is a clear positive trend in the frequency of some types of ridges, like the ridge with axis from the IP to Scandinavia and also in the zonal flow for ERA40 whereas negative trends are observed in the Euro-Atlantic blocking.

Concerning the persistence, CGCM2 simulation is the most persistent (3.61 days) whereas HADCM3 is the less persistent (2.85 days) and present a large number of 1-day events, more than 100 days comparing with ERA40.

Preferred paths for transition between specific CTs have been found. Only all the transitions are available for HADCM3. One of the most likely transitions for ERA40 takes place between the ridge with axis from the IP to Scandinavia to zonal flow. The Atlantic ridges tend to be followed by the positive phase of NAO or lead to some sort of blocking or zonal flow.

8.2. 2071-2100 (SRES A2)

As a general rule, there is a reduction in the number of troughs both in western and eastern Europe, and in the number of ridges over Great Britain and a frequent shift of the jet-stream northwards of its normal position. Another important feature is the reduction of the intensity of ridges over Great Britain and of the troughs over the northwest European coast (Huth, 2000). The CGCM2 exhibits stronger zonal features compared with its control simulation. HADCM3 shows an enhancement of the Atlantic ridge southern Iceland and of the ridge over the North Sea.

The behaviour of the relative frequencies of the CTs are similar. In the CGCM2, the range of variation among the relative frequencies is larger than in control simulation contrarily to ECHAM4 simulation. As it was happened in ERA40 and in the control simulations, the most frequent CTs are related with stronger ridges and zonal flow.

The inter-annual variation of the CTs frequency is rather high as it was in ERA40 and the respective control simulations. There is a clear positive trend in the frequency of some types of ridges, like the ridge with axis

from the IP to Scandinavia and also in the zonal flow. Negative trend is observed in the frequency of the NW flow over central and southern Europe (CGCM2) and the frequency of an Atlantic ridge over southern Iceland.

The response of the atmospheric circulation is manifested in a decrease of the mean duration, for CGCM2 and ECHAM4, especially notorious in this latter one. Accordingly, a great number of 1-day events and a small percentage of time spent in the events lasting four days or more is detected. On the contrary, HADCM3 exhibits a considerable increase, more considerable due to the less number of winters taken into consideration. Excepting the ECHAM4 SRES A2 simulation, the mean duration is higher than in ERA40. HADCM3 exhibits the longest event, with a duration of 39 days, (HADCM3_A2_8), linked to an omega-like configuration.

The transitions in the SRES A2 present an extraordinary increase with respect to the 1961-1990 period, especially the evolution from a ridge with axis from IP to Scandinavia to strong zonal flow. These features will deserve a more detailed analysis.

This study proposes the circulation classification method as a useful tool to analyse and validate the climate response of GCMs. Comparisons are particularly focused on (i) shapes of the mean type patterns, (ii) the frequency and persistence of the types and iii) transitions between CTs.

ANNEXES

I. Figures

I.1. Distribution of events: 1961-1990

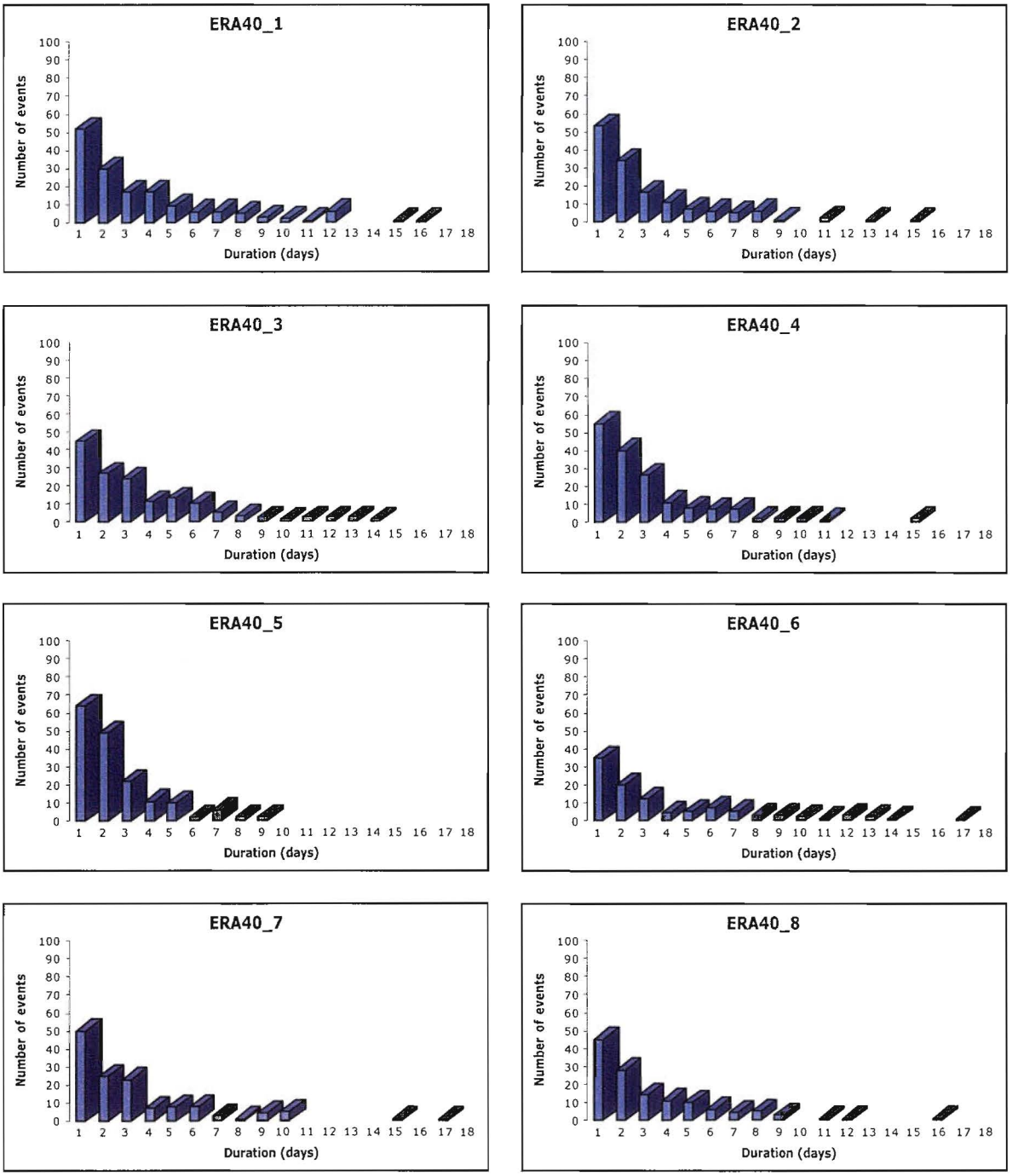

Figure 8. Number of events in each circulation type as a function of the duration in days for ERA40 over the period DJFM 1961-1990.

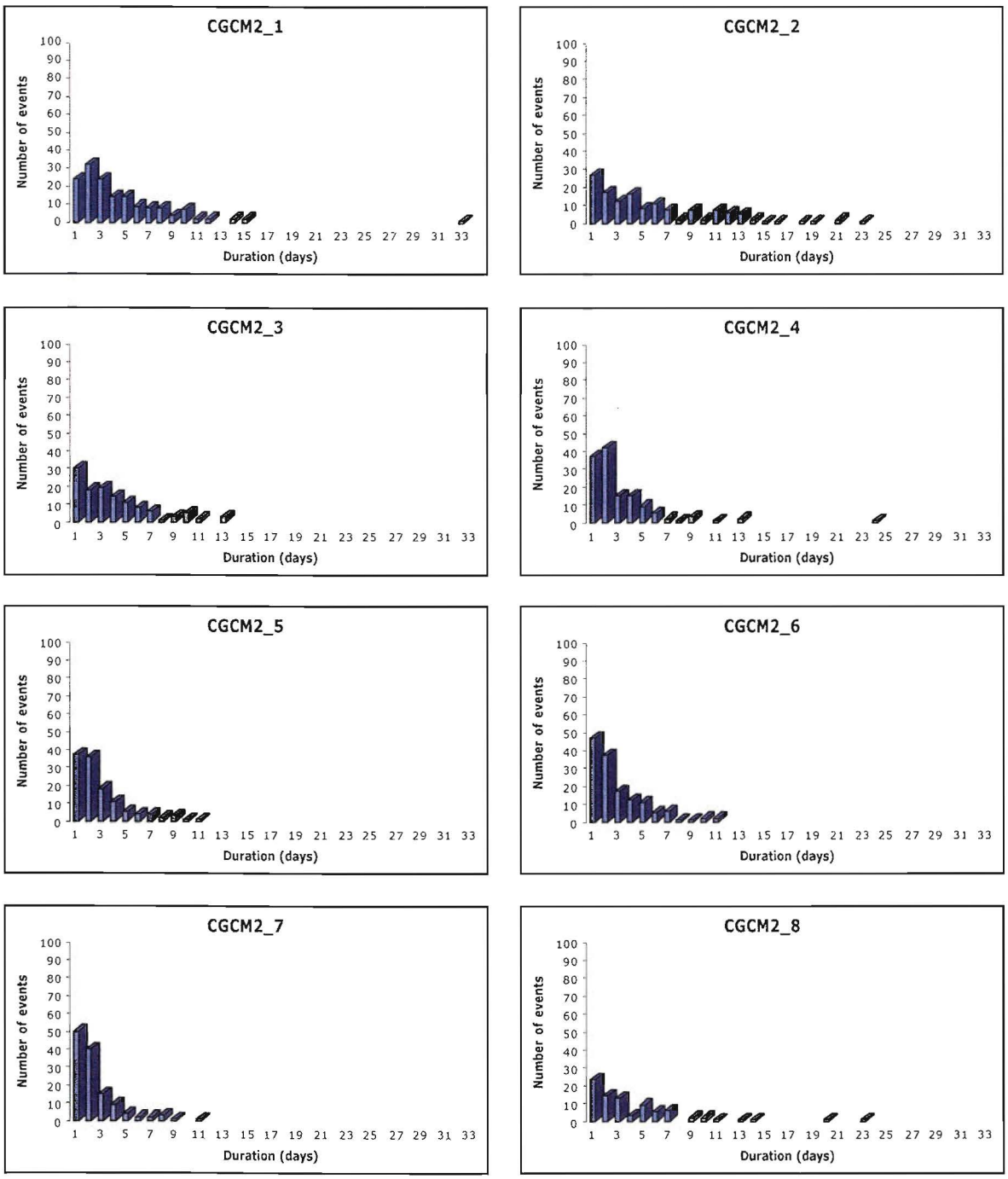

Figure 9. Number events in each circulation type as a function of the duration in days for CGCM2 over the period DJFM 1961-1990.

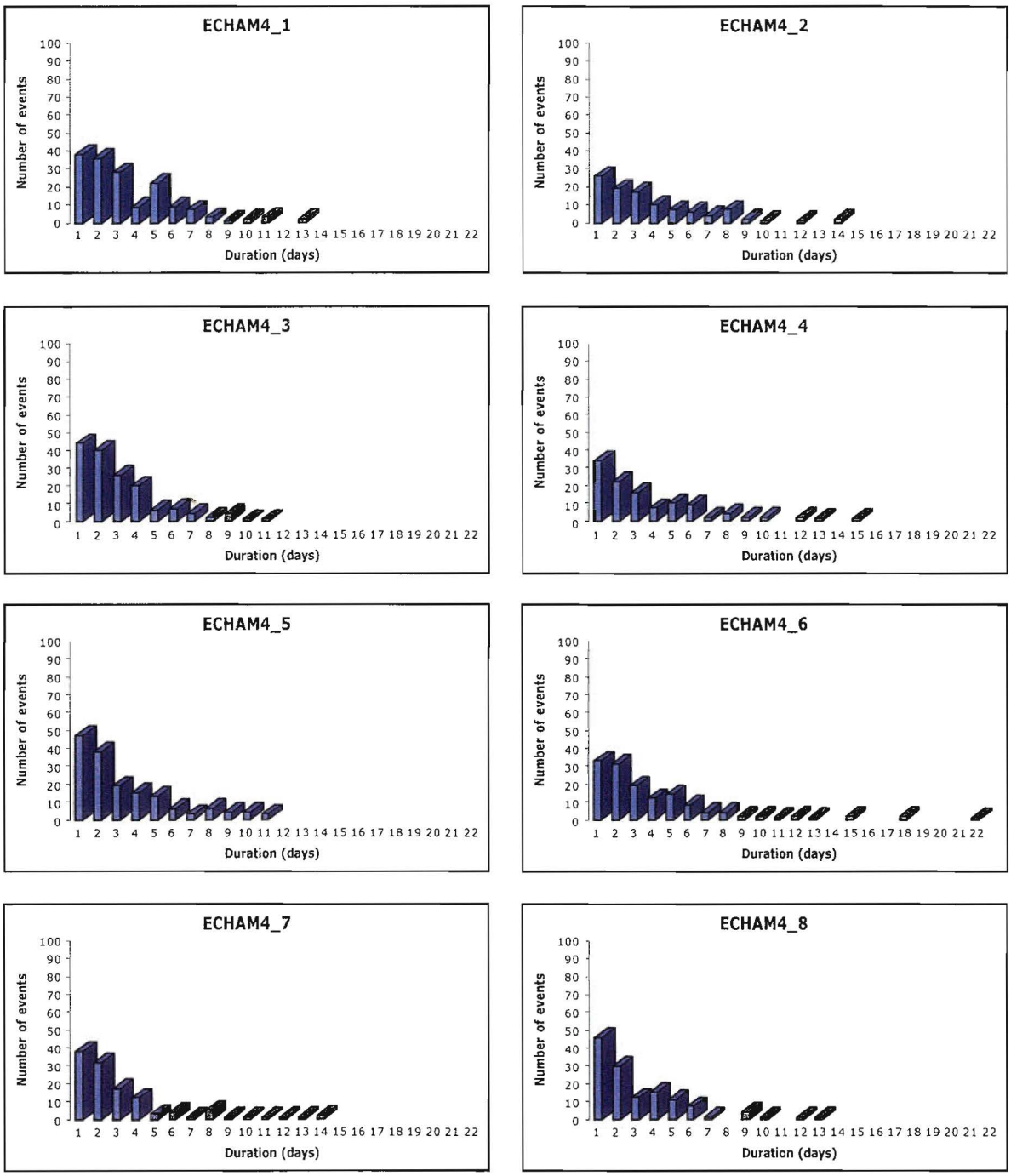

Figure 10. Number of events in each circulation type as a function of the duration in days for ECHAM4 over the period DJFM 1961-1990.

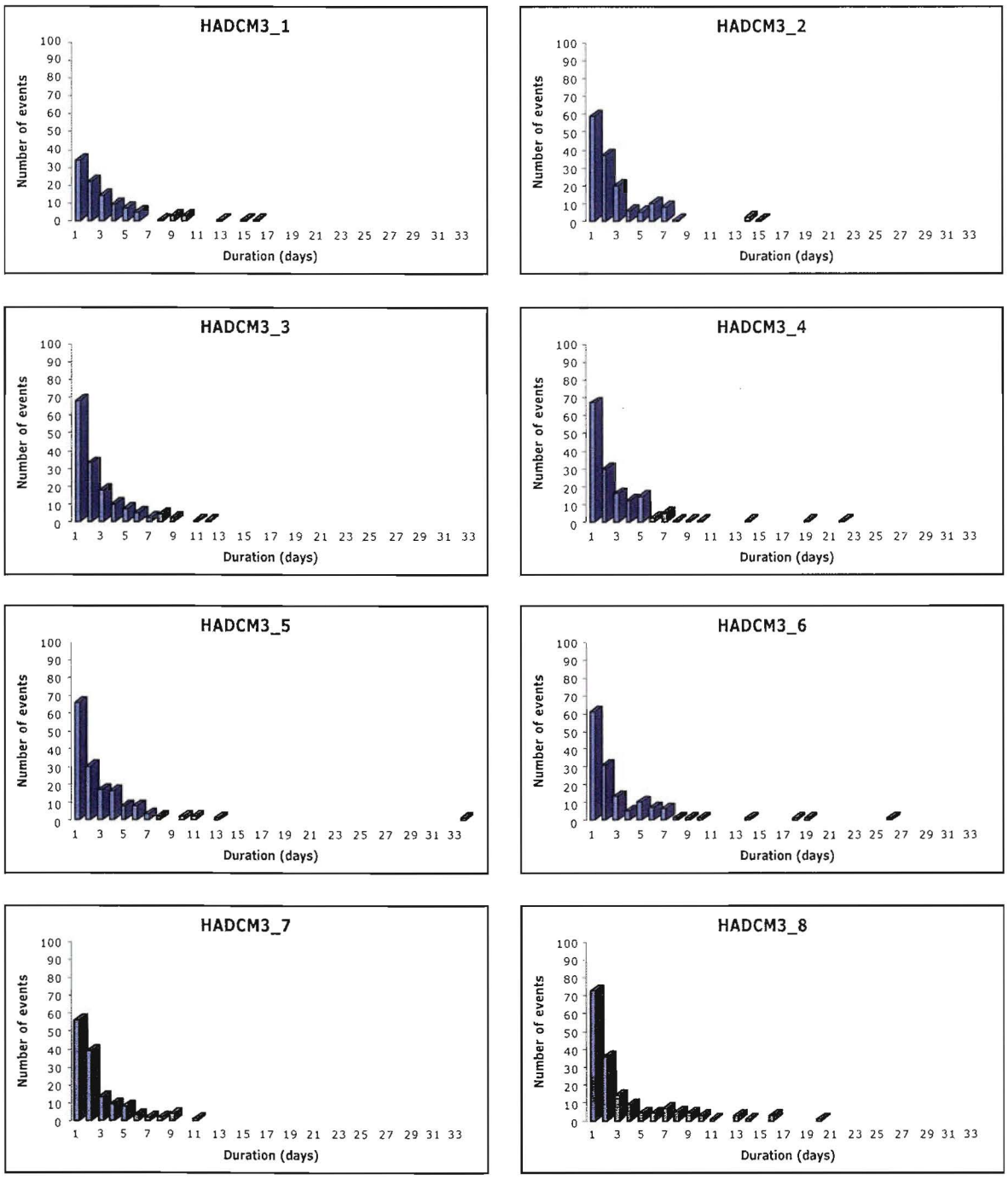

Figure 11. Number of events in each circulation type as a function of the duration in days for HADCM3 over the period DJFM 1961-1989.

I.2. Distribution of events: 2071-2100 (SRES A2)

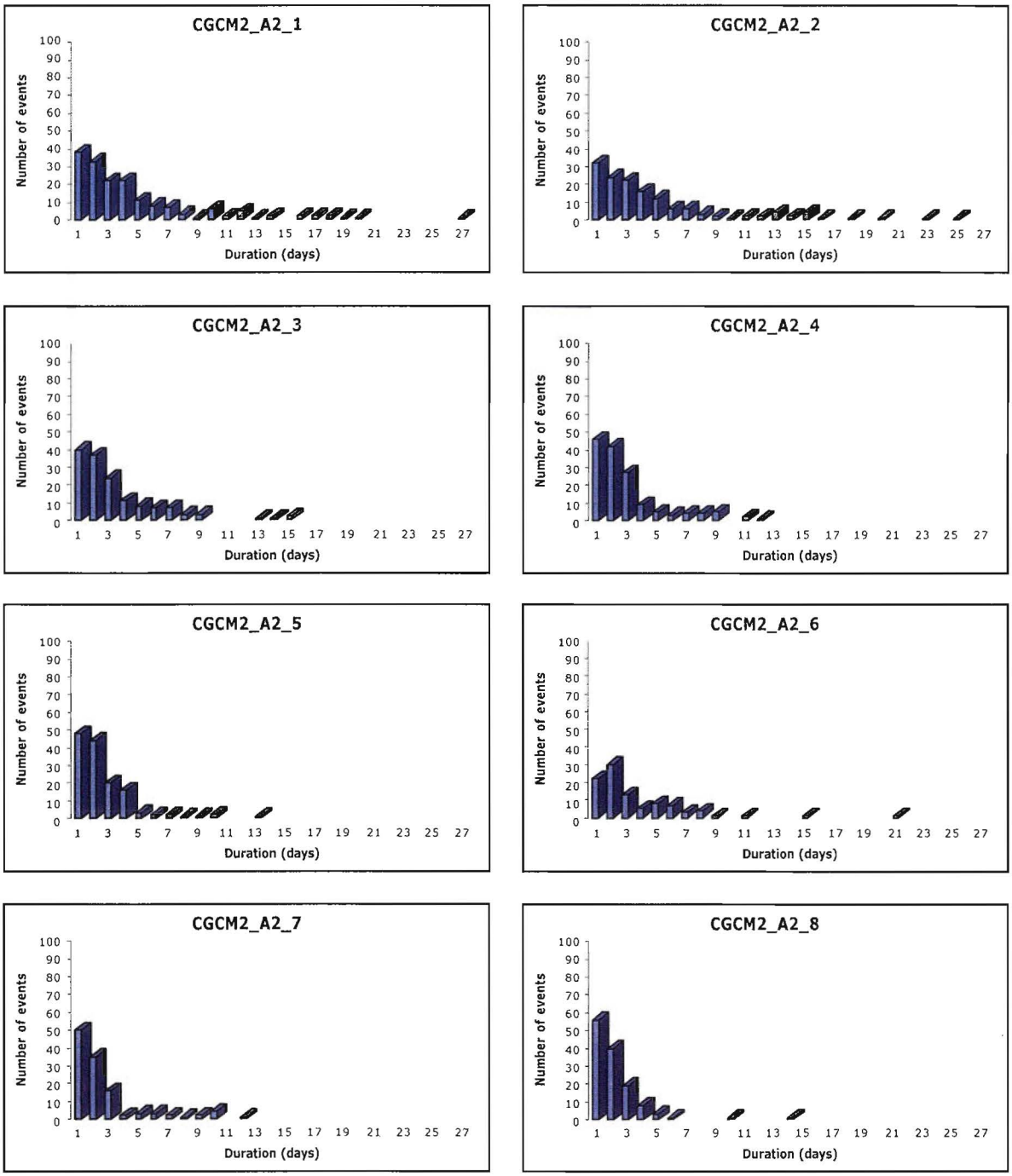

Figure 15. Number of events in each circulation type as a function of the duration in days for CGCM2 over the period DJFM 2071-2100.

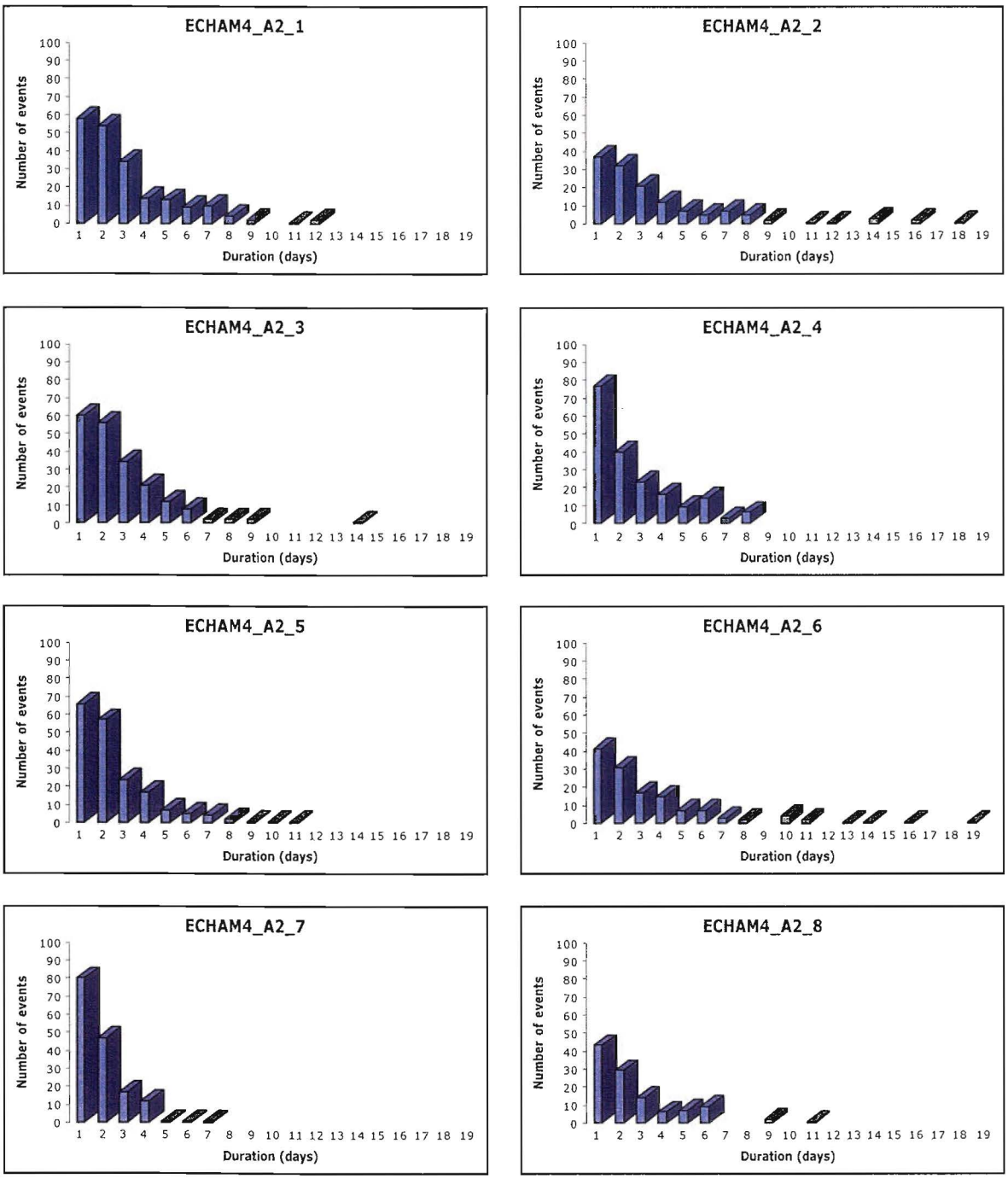

Figure 16. Number of events in each circulation type as a function of the duration in days for ECHAM4 over the period DJFM 2071-2100.

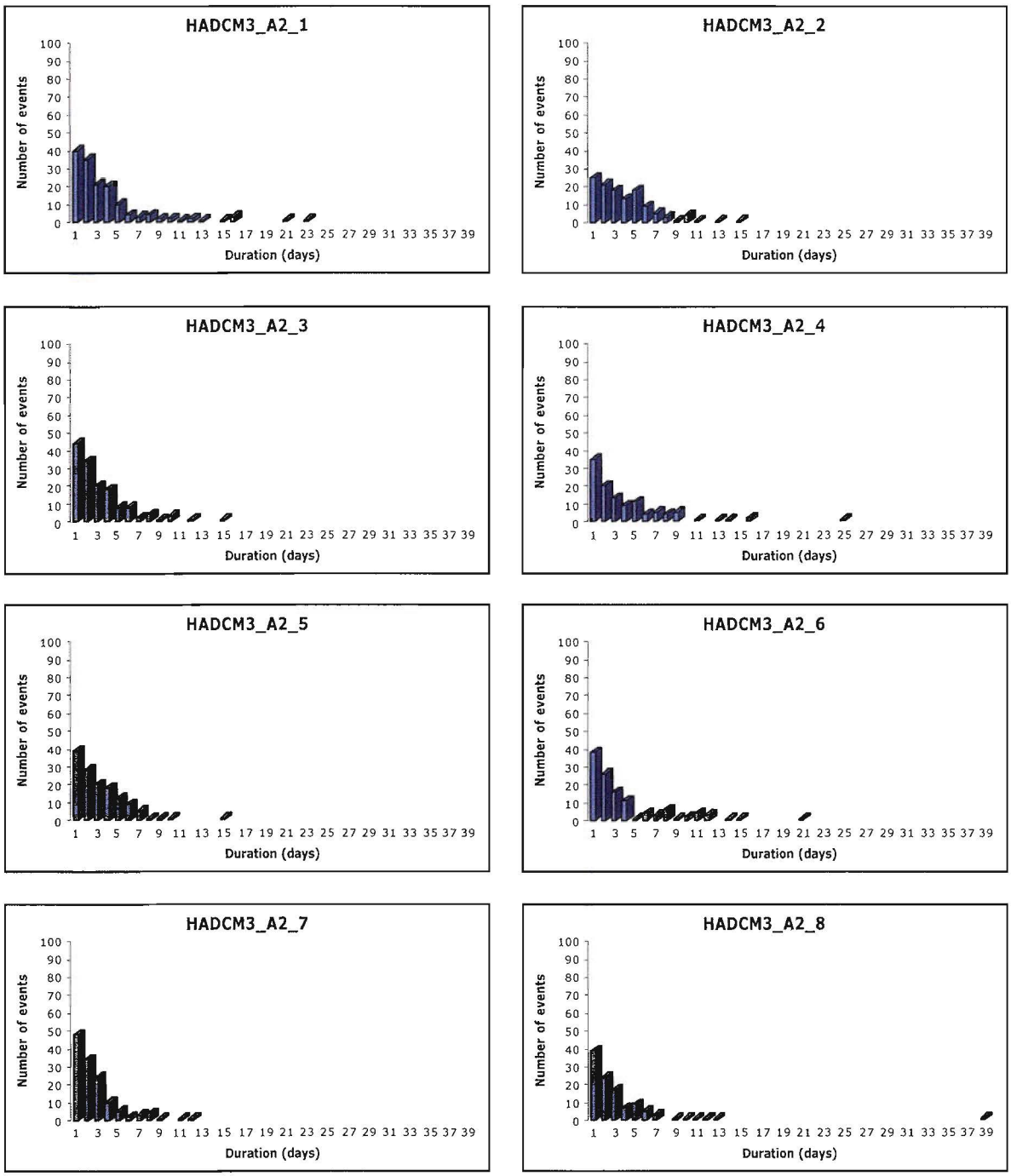

Figure 17. Number of events in each circulation type as a function of the duration in days for HADCM3 over the period DJFM 2071-2099.

I.3. Trends in the Circulation Types frequency: 1961-1990

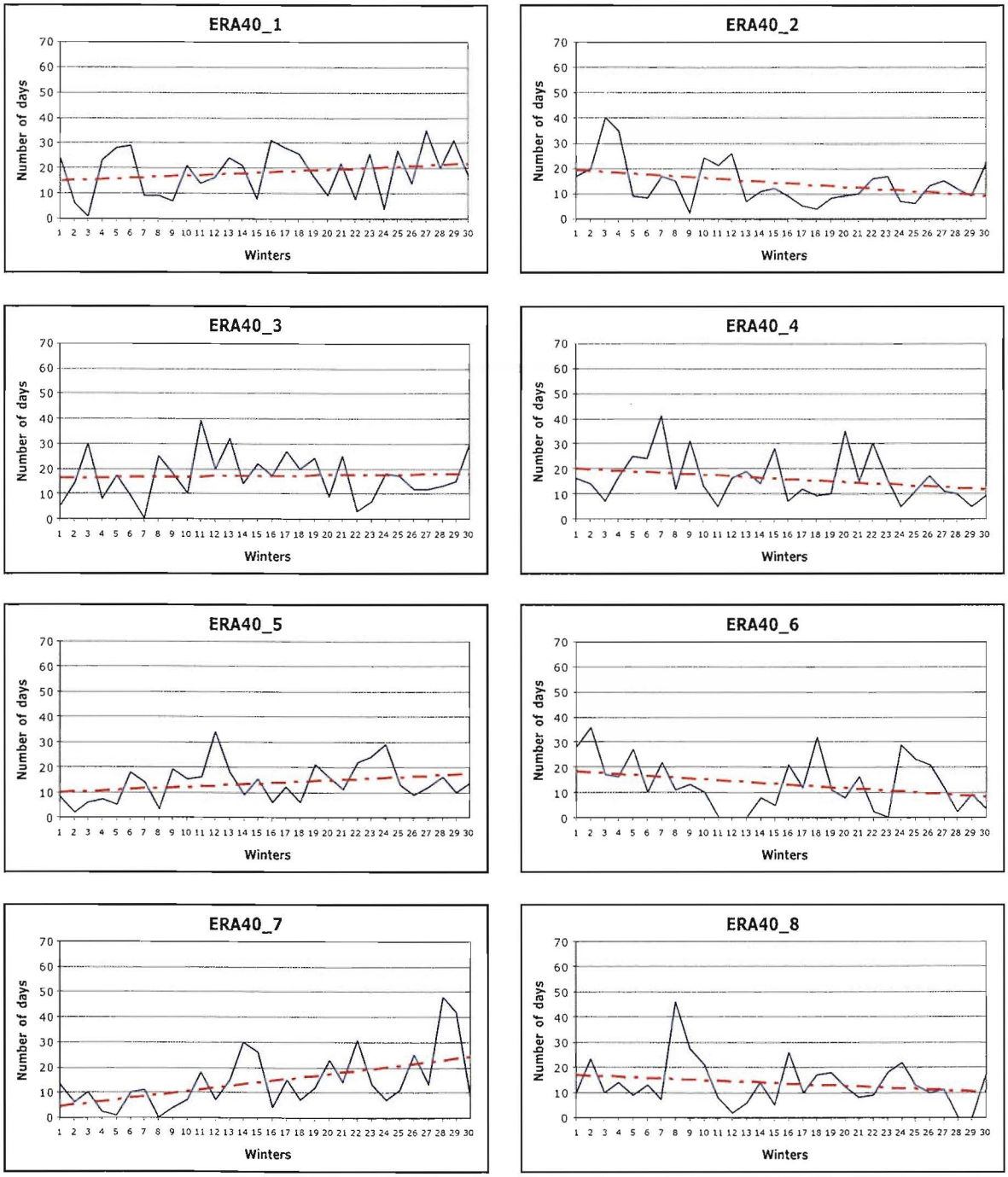

Figure 18. Number of days classified for each circulation type per winter for ERA40. The red line corresponds to a linear trend.

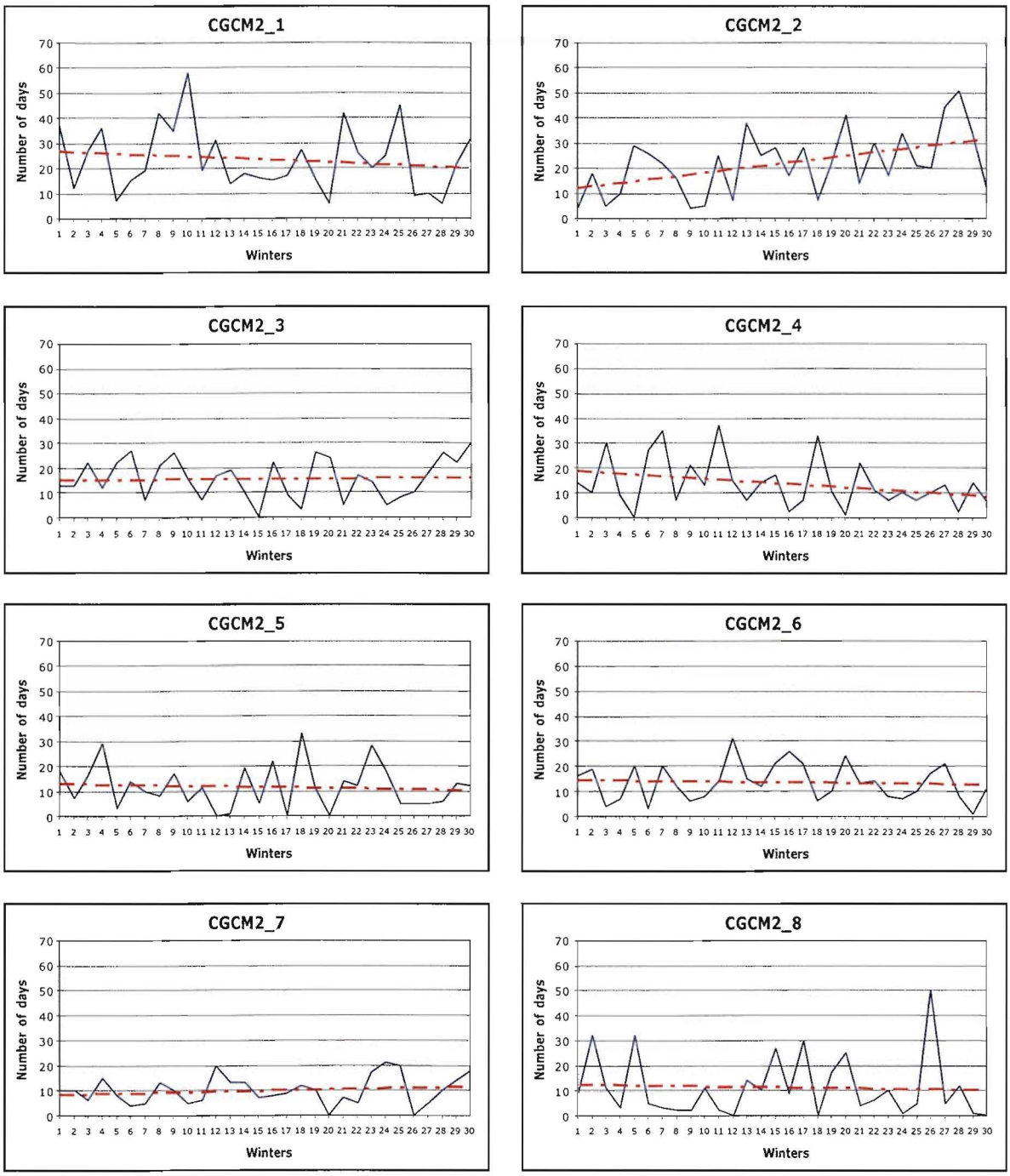

Figure 19. Number of days classified for each circulation type per winter for CGCM2 over the period 1961-1990. The red line corresponds to a linear trend.

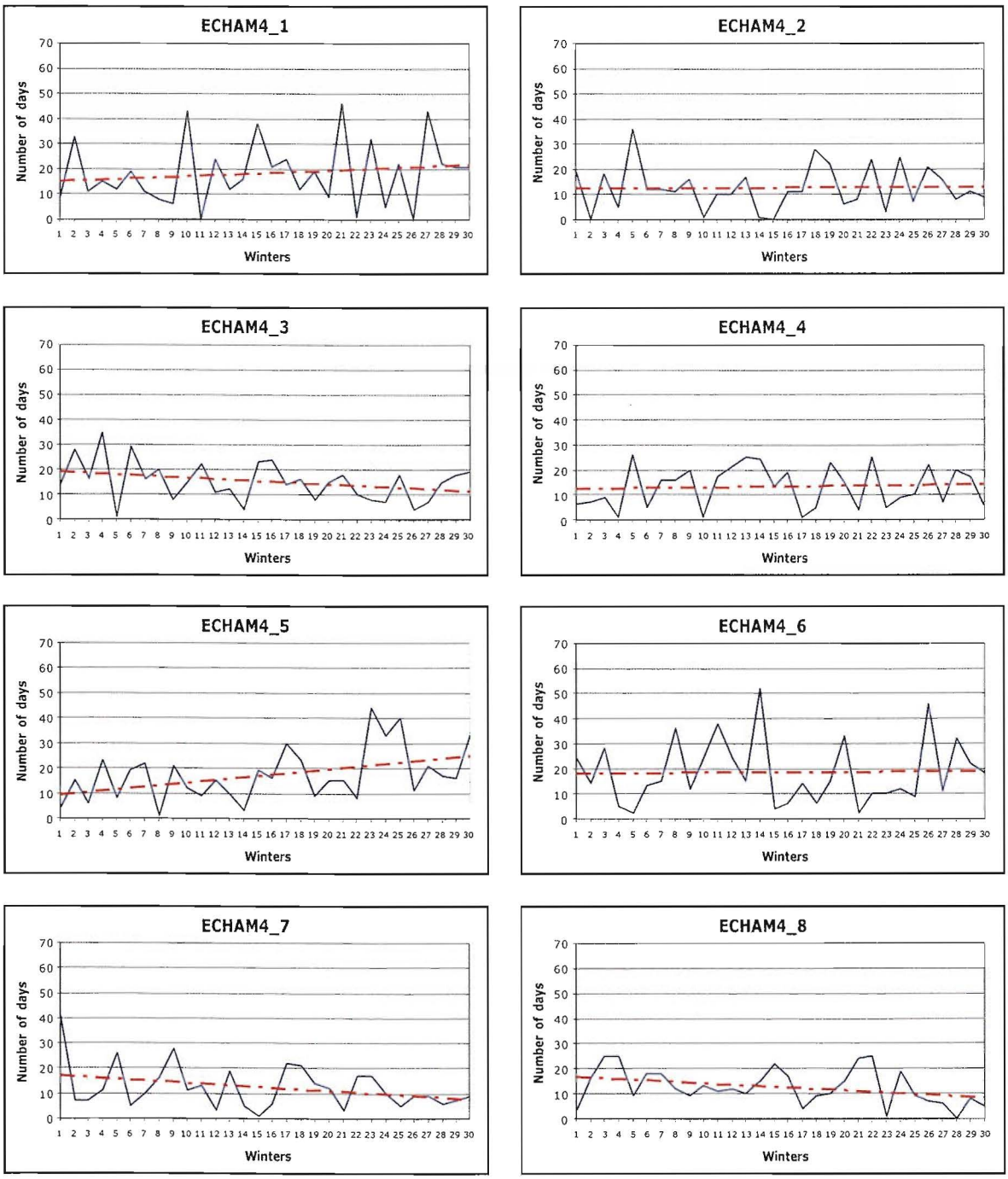

Figure 20. Number of days classified for each circulation type per winter for ECHAM4 over the period 1961-1990. The red line corresponds to a linear trend.

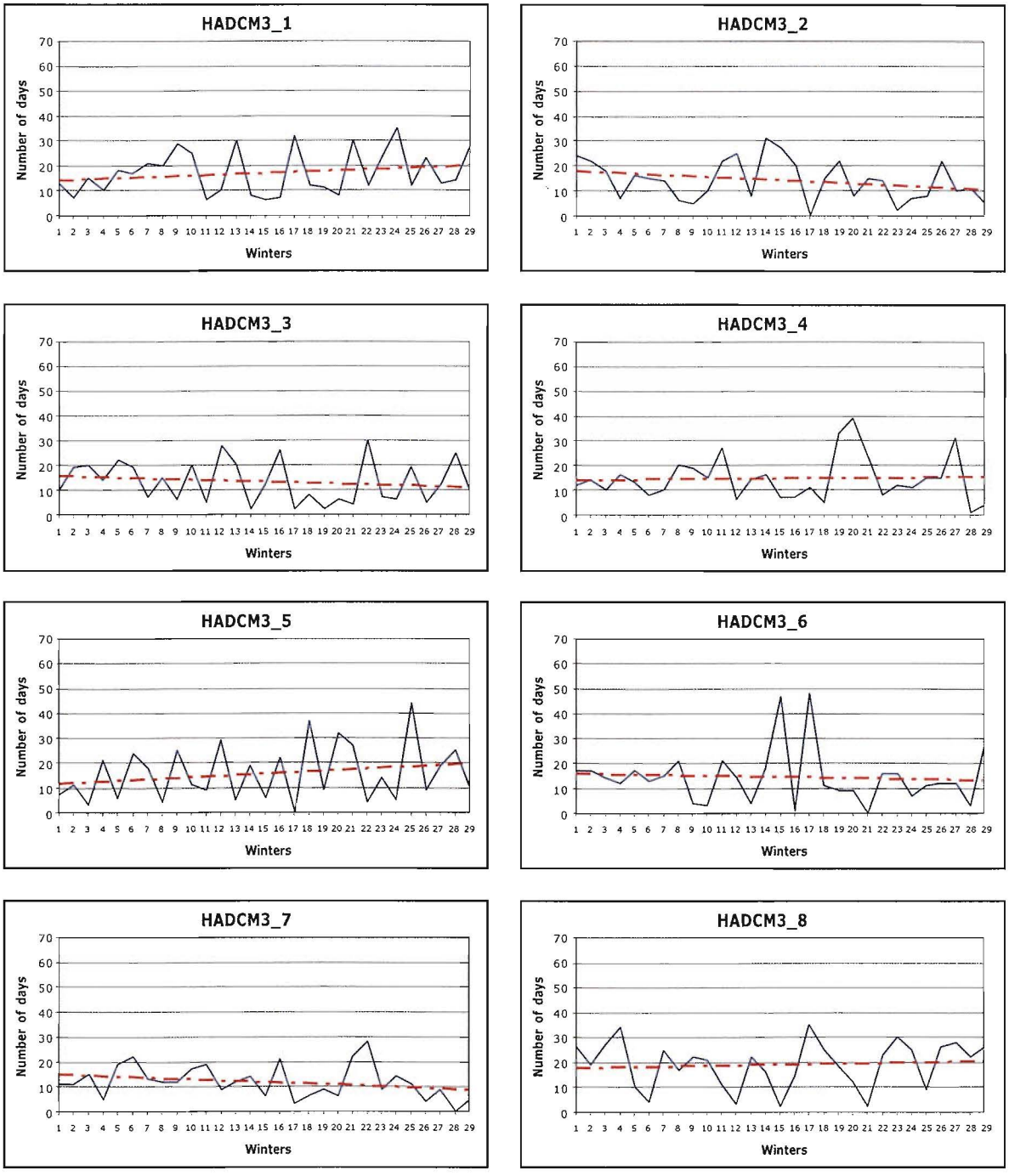

Figure 21. Number of days classified for each circulation type per winter for HADCM3 over the period 1961-1989. The red line corresponds to a linear trend.

I.4. Trends in the Circulation Types frequency: 2071-2100 (SRES A2)

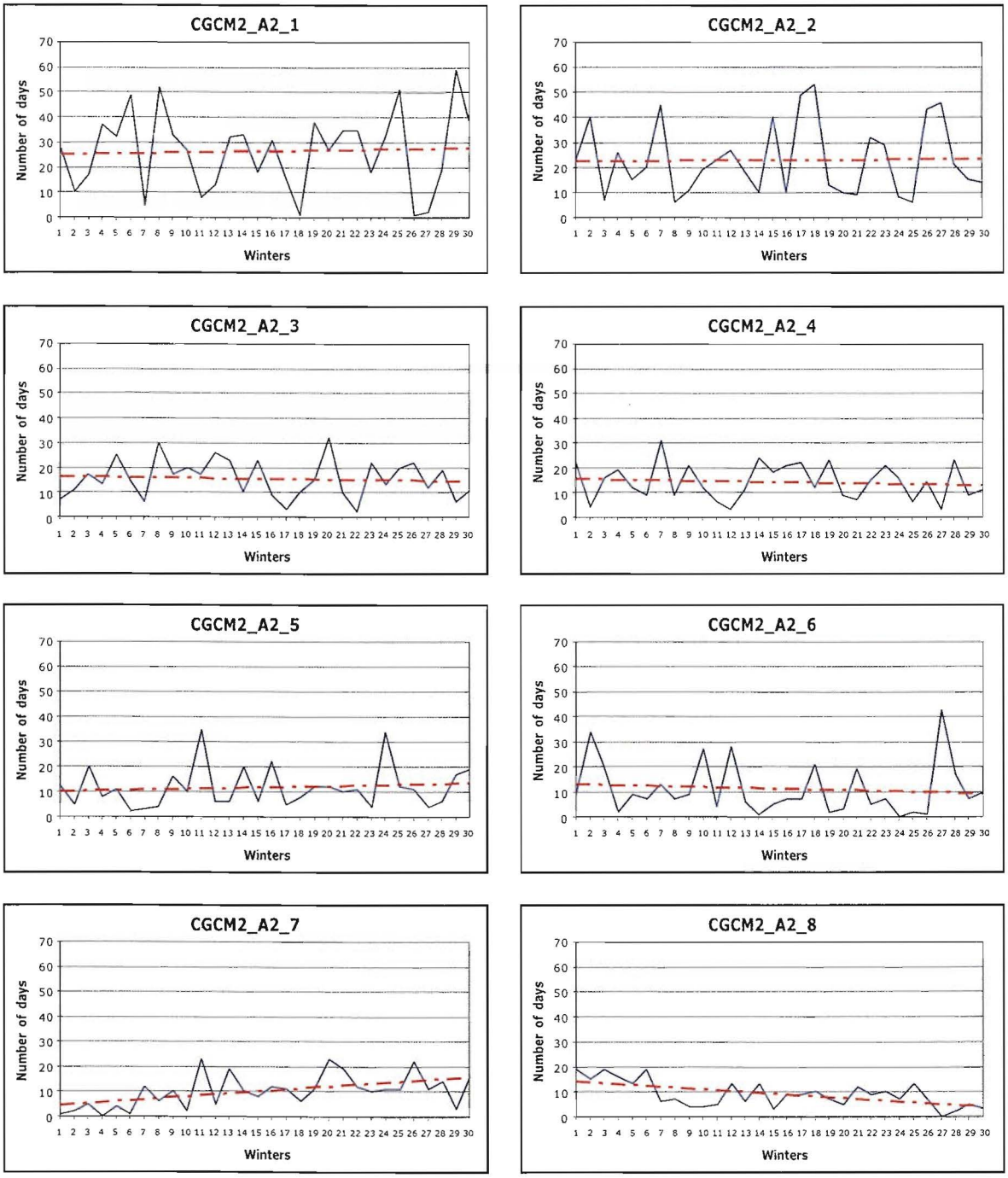

Figure 22. Number of days classified for each circulation type per winter for CGCM2 over the period 2071-2100. The red line corresponds to a linear trend.

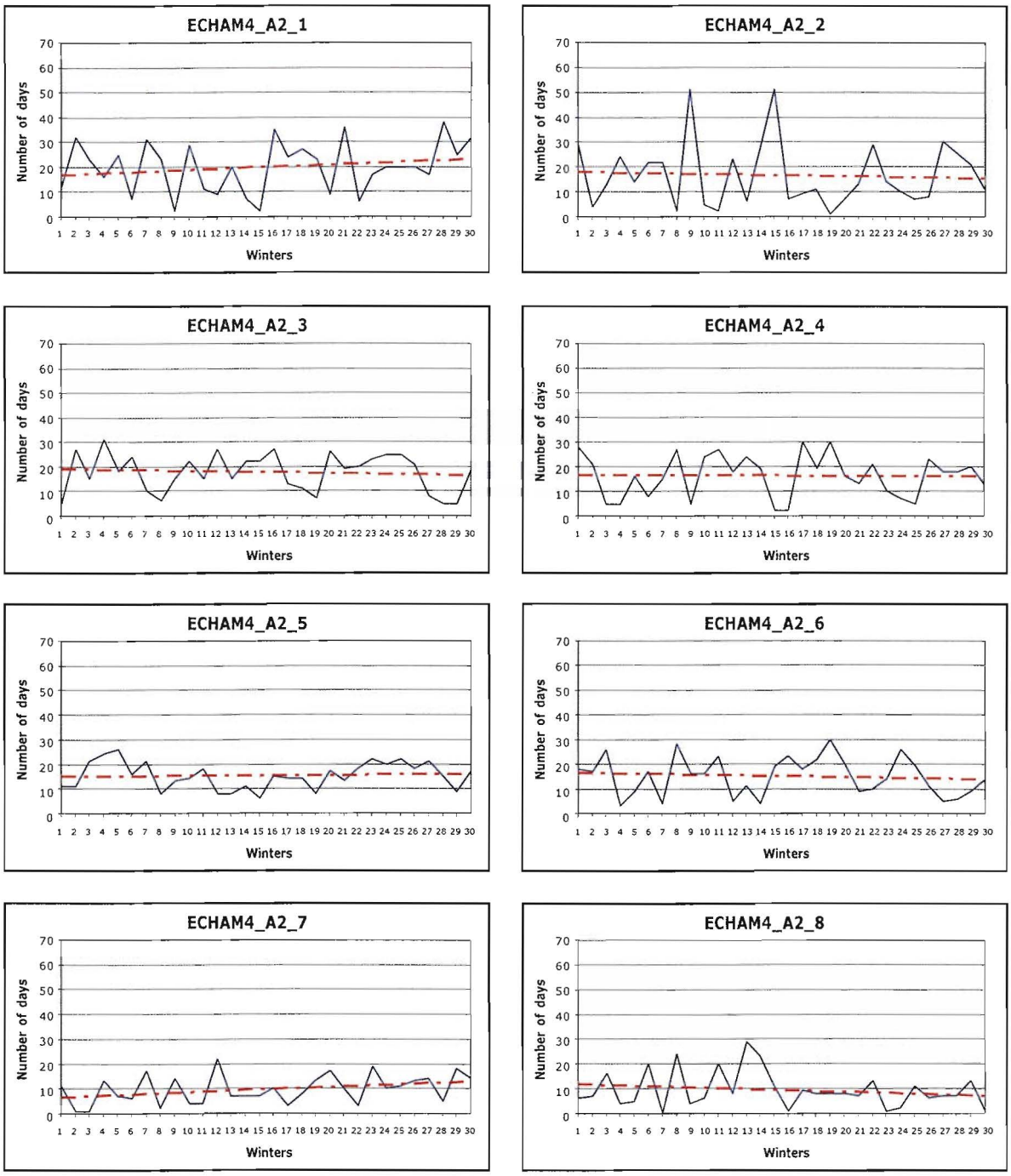

Figure 23. Number of days classified for each circulation type per winter for ECHAM4 over the period 2071-2100. The red line corresponds to a linear trend.

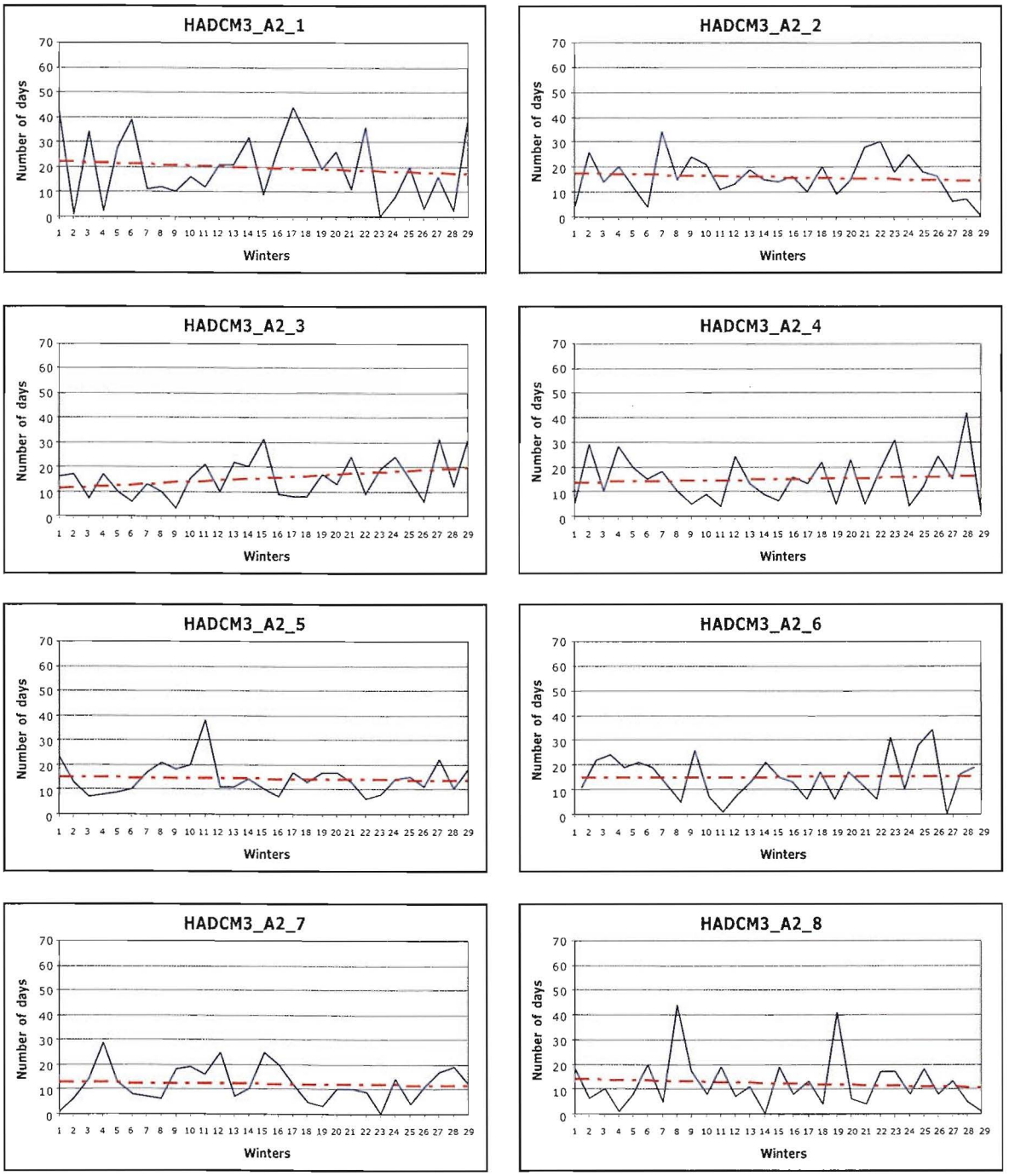

Figure 24. Number of days classified for each circulation type per winter for HADCM3 over the period 2071-2099. The red line corresponds to a linear trend.

II. Tables

ERA40		CGCM2		ECHAM4		HADCM3	
ERA40_1	15.29	CGCM2_1	19.37	ECHAM4_1	15.42	HADCM3_1	14.25
ERA40_2	11.73	CGCM2_2	17.99	ECHAM4_2	10.50	HADCM3_2	11.75
ERA40_3	14.13	CGCM2_3	12.95	ECHAM4_3	12.64	HADCM3_3	10.92
ERA40_4	13.30	CGCM2_4	11.32	ECHAM4_4	10.94	HADCM3_4	12.13
ERA40_5	11.29	CGCM2_5	9.59	ECHAM4_5	14.42	HADCM3_5	13.07
ERA40_6	11.13	CGCM2_6	11.18	ECHAM4_6	15.33	HADCM3_6	12.07
ERA40_7	11.90	CGCM2_7	8.29	ECHAM4_7	10.28	HADCM3_7	9.89
ERA40_8	11.21	CGCM2_8	9.31	ECHAM4_8	10.47	HADCM3_8	15.92

Table 2. Relative frequency of occurrence (%) of the different circulation types over the period DJFM 1961-1990.

ERA40		CGCM2		ECHAM4		HADCM3	
ERA40_1	3.56	CGCM2_1	4.59	ECHAM4_1	3.47	HADCM3_1	2.99
ERA40_2	2.98	CGCM2_2	5.14	ECHAM4_2	3.71	HADCM3_2	2.74
ERA40_3	3.47	CGCM2_3	3.92	ECHAM4_3	2.94	HADCM3_3	2.52
ERA40_4	2.96	CGCM2_4	3.09	ECHAM4_4	3.52	HADCM3_4	2.78
ERA40_5	2.44	CGCM2_5	2.85	ECHAM4_5	3.28	HADCM3_5	2.92
ERA40_6	3.88	CGCM2_6	2.88	ECHAM4_6	4.00	HADCM3_6	3.00
ERA40_7	3.18	CGCM2_7	2.37	ECHAM4_7	3.11	HADCM3_7	2.51
ERA40_8	3.16	CGCM2_8	4.12	ECHAM4_8	2.92	HADCM3_8	3.30

Table 3. Mean persistence (days) over the period DJFM 1961-1990.

CGCM2		ECHAM4		HADCM3	
CGCM2_A2_1	21.87	ECHAM4_A2_1	16.61	HADCM3_A2_1	16.46
CGCM2_A2_2	18.95	ECHAM4_A2_2	13.86	HADCM3_A2_2	13.33
CGCM2_A2_3	12.81	ECHAM4_A2_3	14.67	HADCM3_A2_3	12.76
CGCM2_A2_4	11.82	ECHAM4_A2_4	13.56	HADCM3_A2_4	12.53
CGCM2_A2_5	9.67	ECHAM4_A2_5	12.75	HADCM3_A2_5	12.01
CGCM2_A2_6	9.15	ECHAM4_A2_6	12.56	HADCM3_A2_6	12.61
CGCM2_A2_7	8.29	ECHAM4_A2_7	8.08	HADCM3_A2_7	10.06
CGCM2_A2_8	7.43	ECHAM4_A2_8	7.92	HADCM3_A2_8	10.23

Table 5. Relative frequency of occurrence (%) of the different circulation types over the period DJFM 2071-2100.

CGCM2		ECHAM4		HADCM3	
CGCM2_A2_1	4.67	ECHAM4_A2_1	2.98	HADCM3_A2_1	3.79
CGCM2_A2_2	4.81	ECHAM4_A2_2	3.96	HADCM3_A2_2	3.87
CGCM2_A2_3	3.23	ECHAM4_A2_3	2.67	HADCM3_A2_3	3.08
CGCM2_A2_4	2.90	ECHAM4_A2_4	2.60	HADCM3_A2_4	3.89
CGCM2_A2_5	2.51	ECHAM4_A2_5	2.48	HADCM3_A2_5	3.10
CGCM2_A2_6	3.46	ECHAM4_A2_6	3.40	HADCM3_A2_6	3.72
CGCM2_A2_7	2.53	ECHAM4_A2_7	1.83	HADCM3_A2_7	2.63
CGCM2_A2_8	2.09	ECHAM4_A2_8	2.57	HADCM3_A2_8	3.24

Table 6. Mean persistence (days) over the period 2071-2100.

	ERA40	CGCM2	ECHAM4	HADCM3
M	3.16	3.61	3.36	2.85
≥4	62.34	68.43	64.89	58.22
1	399	275	306	515

Table 4. Characteristics of duration of events: mean duration in days (M), percentage of time spent in the events lasting 4 days or more and the number of 1-day events over the period DJFM 1961-1990.

	CGCM2	ECHAM4	HADCM3
M	3.33	2.75	3.40
≥4	61.68	55.11	65.55
1	332	462	308

Table 7. Characteristics of duration of events: mean duration in days (M), percentage of time spent in the events lasting 4 days or more and the number of 1-day events over the period DJFM 2071-2100.

From/To	ERA40_1	ERA40_2	ERA40_3	ERA40_4	ERA40_5	ERA40_6	ERA40_7	ERA40_8
ERA40_1	-	0.65	19.23	18.57	16.67	8.98	13.47	22.44
ERA40_2	0.0	-	16.20	21.83	18.31	16.91	17.61	9.16
ERA40_3	18.25	15.54	-	0.0	30.41	10.81	9.46	15.54
ERA40_4	16.67	18.52	0.0	-	16.05	10.50	25.93	12.35
ERA40_5	16.77	19.76	16.17	19.76	-	0.0	11.98	15.57
ERA40_6	26.22	9.71	22.33	17.48	0.0	-	13.60	10.68
ERA40_7	27.95	8.83	19.86	24.27	13.24	5.89	-	0.0
ERA40_8	7.04	25.79	14.07	14.07	20.32	18.75	0.0	-

Table 8. Frequency of the transitions from a circulation type (rows) to a different circulation type (columns) (in %) for the ERA40 classification over the period DJFM 1961-1990.

From/To	CGCM2_1	CGCM2_2	CGCM2_3	CGCM2_4	CGCM2_5	CGCM2_6	CGCM2_7	CGCM2_8
CGCM2_1	-	1.31	15.04	28.11	17.65	20.27	7.85	9.81
CGCM2_2	0.0	-	26.05	18.49	10.93	15.13	20.17	9.25
CGCM2_3	16.67	18.34	-	0.0	10.84	25.00	13.34	15.84
CGCM2_4	24.25	8.34	0.0	-	31.06	10.61	15.91	9.85
CGCM2_5	27.87	15.58	14.76	13.12	-	1.64	26.23	0.82
CGCM2_6	13.58	23.58	16.43	15.00	0.0	-	15.00	16.43
CGCM2_7	31.75	7.94	8.73	19.05	15.88	16.67	-	0.0
CGCM2_8	9.76	26.83	17.08	7.32	9.76	29.27	0.00	-

Table 9. Frequency of the transitions from a circulation type (rows) to a different circulation type (columns) (in %) for the CGCM2 classification over the period DJFM 1961-1990.

From/To	ECHAM4_1	ECHAM4_2	ECHAM4_3	ECHAM4_4	ECHAM4_5	ECHAM4_6	ECHAM4_7	ECHAM4_8
ECHAM4_1	-	0.0	8.75	16.88	30.00	12.50	11.88	20.00
ECHAM4_2	0.0	-	20.00	16.00	21.00	13.00	14.00	16.00
ECHAM4_3	30.52	11.69	-	0.0	17.54	12.34	8.45	19.48
ECHAM4_4	7.28	9.09	0.0	-	20.00	30.00	17.28	16.37
ECHAM4_5	17.84	15.29	26.76	8.92	-	0.0	12.74	18.48
ECHAM4_6	23.19	13.05	18.12	18.12	0.73	-	23.92	2.90
ECHAM4_7	11.02	19.50	13.56	12.72	21.19	22.04	-	0.0
ECHAM4_8	24.81	5.43	28.69	10.08	10.08	20.93	0.0	-

Table 10. Frequency of the transitions from a circulation type (rows) to a different circulation type (columns) (in %) for the ECHAM4 classification over the period DJFM 1961-1990.

From/To	HADCM3_1	HADCM3_2	HADCM3_3	HADCM3_4	HADCM3_5	HADCM3_6	HADCM3_7	HADCM3_8
HADCM3_1	-	5.53	12.89	15.95	16.57	14.73	19.64	14.73
HADCM3_2	8.28	-	13.11	15.18	15.18	16.56	14.49	17.25
HADCM3_3	15.24	14.57	-	4.64	18.55	18.55	11.92	16.56
HADCM3_4	14.00	17.34	6.00	-	21.34	9.34	13.34	18.67
HADCM3_5	17.95	18.59	23.72	14.11	-	0.65	8.34	16.67
HADCM3_6	15.95	15.95	13.05	11.60	1.45	-	19.57	22.47
HADCM3_7	14.60	16.79	15.33	21.17	15.33	12.41	-	4.38
HADCM3_8	21.82	8.49	15.76	16.97	14.55	18.79	3.64	-

Table 11. Frequency of the transitions from a circulation type (rows) to a different circulation type (columns) (in %) for the HADCM3 classification over the period DJFM 1961-1989.

From/To	CGCM2_1	CGCM2_2	CGCM2_3	CGCM2_4	CGCM2_5	CGCM2_6	CGCM2_7	CGCM2_8
CGCM2_1	-	1.18	12.95	27.65	15.89	12.95	10.00	19.42
CGCM2_2	0.0	-	19.58	19.58	16.09	19.58	13.99	11.19
CGCM2_3	29.17	13.89	-	1.39	11.12	11.12	29.87	3.48
CGCM2_4	17.57	20.27	0.0	-	25.00	4.06	5.41	27.71
CGCM2_5	41.73	10.80	13.67	12.23	-	0.72	7.20	13.67
CGCM2_6	8.34	21.88	12.50	21.88	0.0	-	20.84	14.59
CGCM2_7	14.41	23.73	11.02	22.89	17.80	9.33	-	0.85
CGCM2_8	14.73	20.16	38.76	4.66	12.41	9.31	0.0	-

Table 12. Frequency of the transitions from a circulation type (rows) to a different circulation type (columns) (in %) for the CGCM2 classification over the period DJFM 2071-2100.

From/To	ECHAM4_1	ECHAM4_2	ECHAM4_3	ECHAM4_4	ECHAM4_5	ECHAM4_6	ECHAM4_7	ECHAM4_8
ECHAM4_1	-	1.00	8.50	41.00	26.50	7.00	6.50	9.50
ECHAM4_2	0.74	-	41.18	2.95	12.50	12.50	21.33	8.83
ECHAM4_3	24.37	11.17	-	0.0	9.65	27.42	23.86	3.50
ECHAM4_4	19.68	21.28	1.07	-	20.22	7.45	10.64	19.68
ECHAM4_5	21.63	15.14	30.81	13.52	-	1.09	6.49	11.36
ECHAM4_6	19.85	10.69	8.40	20.61	0.0	-	29.01	11.45
ECHAM4_7	18.24	13.21	25.79	6.29	34.60	1.89	-	0.0
ECHAM4_8	17.12	8.11	11.72	35.14	2.71	25.23	0.0	-

Table 13. Frequency of the transitions from a circulation type (rows) to a different circulation type (columns) (in %) for the ECHAM4 classification over the period DJFM 2071-2100.

From/To	HADCM3_1	HADCM3_2	HADCM3_3	HADCM3_4	HADCM3_5	HADCM3_6	HADCM3_7	HADCM3_8
HADCM3_1	-	0.0	11.26	20.53	17.88	13.91	28.48	7.95
HADCM3_2	1.74	-	23.48	18.26	23.48	9.57	13.05	10.44
HADCM3_3	19.86	9.22	-	0.0	28.37	9.93	14.19	18.44
HADCM3_4	11.01	12.85	0.0	-	13.77	28.44	19.27	14.68
HADCM3_5	27.41	20.00	7.41	13.34	-	0.74	9.63	21.49
HADCM3_6	16.67	17.55	24.57	14.04	0.88	-	17.55	8.78
HADCM3_7	21.22	25.76	12.88	10.61	13.64	14.40	-	1.52
HADCM3_8	23.37	6.55	38.32	8.42	6.55	16.83	0.0	-

Table 14. Frequency of the transitions from a circulation type (rows) to a different circulation type (columns) (in %) for the HADCM3 classification over the period DJFM 2071-2099.

REFERENCES

ACHATZ U, JD OPSTEEGH (2003). Primitive-equation-based low-order models with seasonal cycle, Part II: Application to complexity and nonlinearity of large-scale atmospheric dynamics. *J Atmos Sci,* 60: 478-490.

BARTZOKAS A, DA METAXAS (1996). Northern Hemisphere gross circulation types. Climatic change and temperature distribution. *Meteorologische Zeitschrift,* NF 5: 99-109.

BATES GT, GA MEEHL (1986). The effect of CO_2 concentration on the frequency of blocking in a general circulation model coupled to a simple mixed layer ocean model. *Mon Wea Rev,* 114: 687-701.

BLACKMON ML, YH LEE, JM WALLACE (1984). Horizontal structure of 500 mb height fluctuations with long, intermediate, and short time scales. *J Atmos Sci,* 41: 961-979.

BRANDERFELT J (2006). Atmospheric modes of variability in a changing climate. *J Climate,* 19: 5934-5943.

BRANDERFELT J, E KALLEN (2004). The response of the southern hemisphere circulation to an enhanced greenhouse gas forcing. *J Climate,* 17: 4425-4442.

CARNELL RE, CA SENIOR, JFB MITCHELL (1996). An assessment of measures of storminess: Simulated changes in northern hemisphere winter due to increasing CO_2. *Climate Dyn,* 12: 467-476.

CASADO MJ, MA PASTOR, FJ DOBLAS-REYES (2007). Euro-Atlantic types and modes of variability in winter. Submitted to *Theor Appl Climatol.*

CASSOU C, L TERRAY, JM HURRELL, C DESER (2004). North Atlantic winter climate regimes: Spatial asymmetry, stationarity with time, and oceanic forcing. *J Climate,* 17: 1055-1068.

CHEN WY, HM VAN DEN DOOL (1995). Low-frequency anomalies in the NMC MRF model and reality. *J Climate,* 8: 1369-1385.

CHENG X, TJ DUNKERTON (1995). Orthogonal rotation of spatial patterns derived from singular value decomposition analysis. *J Climate,* 8: 2631-2643.

COMPAGNUCCI RH, MA SALLES (1997). Surface pressure patterns during the year over Southern South America. *Int J Climatol,* 17: 635-653.

DÉQUÉ M, JP PIEDELIEVRE (1995). High resolution climate simulation over Europe. *Climate Dyn,* 11: 321-339.

DOBLAS-REYES FJ, MJ CASADO, MA PASTOR (2002). Seasonal evolution of Northern Hemisphere blocking frequency to the detection index. *J Geophys Res,* 107, D2 10.1029/2000JD290L07202.

FLATO GM et al (2000). The Canadian Centre for Climate Modelling and Analysis Global Coupled Model and its Climate. *Climate Dynamics,* 16: 451-467.

GATES et al (1990). Validation of climate models. Climate Change: The IPCC Scientific Assessment. Cambridge University Press, 93-130.

HESS P, H BREZOWSKI (1952). Katalog der Grosswetterlagen Europas. Berichte des Deutschen Wetterdienstes in der US-Zone, 33.

HUTH R (1996). An intercomparison of computer-assisted circulation classification methods. *Int J Climatol,* 16: 893-922.

HUTH R (1997). Continental-Scale circulation in the UKHI GCM. *J Climate,* 10: 1545-1561.

HUTH R (2000). A circulation classification scheme applicable in GCMs studies. *Theor Appl Climatol,* 67: 1-18.

IPCC (2001). Climate Change 2001: The Scientific Basis. Contribution of Working Group I to the Third Assessment Report of the Intergovernmental Panel on Climate Change (IPCC). JT Houghton, Y Ding, DJ Griggs, M Noguer, PJ van der Linden & D Xiaosu (Eds). Cambridge University Press, UK. pp 944.

JAMES PM (2007). An objective classification method for Hess and Brezowsky Grosswetterlagen over Europe. *Theor Appl Climatol,* 88: 17-42.

JIANG N, JE HAY, GW FISHER (2006). Classification of New Zealand Synoptic Weather Types and Relation to the Southern Oscillation Index. *Weather and Climate*, 25: 43-70.

KEY J, RG CRANE (1986). A comparison of synoptic classification schemes based on objective procedures. *J Climatol*, 6: 375-388.

KIDSON JW, IG WATTERSON (1995). A synoptic climatological evaluation of the changes in the CSIRO nine-level model with double CO2 in the New Zealand region. *Int J Climatol*, 15: 1179-1194.

KIRCHHOFER W (1973). Classification of European 500 mb patterns. Arbeitsbericht der Schweizerischen Meteorogischen Zentralanstalt 43.

KYSELÝ J, R HUTH (2006). Changes in atmospheric circulation over Europe detected by objective and subjective methods. *Theor Appl Climatol*, 85: 19-36.

KYSELÝ J, P DOMONKOS (2006). Recent increase in persistence of atmospheric circulation over Europe. Comparison with long term variations since 1881. *Int J Climatol*, 26: 461-483.

LAMB HH (1950). Types and spells of weather around the year in the British Isles: annual trends, seasonal structure of the year singularities. *Quart J Roy Meteor Soc*, 76: 393-429.

LAMBERT SJ (1995). The effect of enhanced greenhouse warming on winter cyclone frequencies and strengths. *J Climate*, 8: 1447-1552.

LUND IA (1963). Map-pattern classification by statistical methods. *J Appl Meteorol*, 2: 56-65.

MCFARLANE NA, GJ BOER, JP BLANCHET, M LAZARE (1992). The Canadian Climate Centre Second-Generation General Circulation Model and Its Equilibrium Climate. *J Climate*, 5, 1013-1044.

MICHELANGELI PA, R VAUTARD, B LEGRAS (1995). Weather regimes: Recurrence and quasi stationarity. *J Atmos Sci*, 52: 1237-1256.

MITCHELL JFB et al (1990). Equilibrium climate change and its implications for the future. *Climate Change: The IPCC Scientific Assessment.* Cambridge University Press, 131-172.

MO K, M GHIL (1987). Statistics and dynamics of persistent anomalies. *J Atm Sci*, 44: 877-901.

MOLTENI F, F KUCHRASKI, S CORTI (2006). On the predictability of flow-regime properties on interannual to interdecadal timescales. In Predictability of Weather and Climate, Cambridge University Press, Cambridge UK.

MURPHY JM (1995). Transient response of the Hadley Centre coupled ocean-atmosphere model to increasing carbon dioxide. Part I: Control climate and flux adjustment. *J Climate*, 8: 36-56.

PALMER TN (1999). A nonlinear dynamical perspective on climate predictions. *J Climate*, 12: 575-591.

PLAUT G, E SIMONNET (2001). Large-scale circulation classification, weather regimes, and local climate over France, the Alps and Western Europe. *Clim Res*, 17: 303-324.

RICHMAN MB (1986). Rotation of principal components. *J Climate*, 6: 293-335.

RICHMAN MB (1999). Relationships between the definition of the hyperplane width to the fidelity of Principal Component Loading Patterns. *J Climate*, 12: 1557-1576.

ROBERTSON AW (2001). Influence of ocean-atmosphere interaction on the Artic Oscillation in two general circulation models. *J Climate*, 14: 3240-3254.

ROECKNER E et al (1992). Simulation of the present-day climate with the ECHAM4 model: impact of model physics and resolution. Max-Planck Institute for Meteorology, Report No. 93, Hamburg, Germany, 171 pp.

ROECKNER E et al (1996). The atmospheric general circulation model ECHAM-4: model description and simulation of present-day climate. Max-Planck Institute for Meteorology, Report No. 218, Hamburg, Germany, 90 pp.

SÁNCHEZ GÓMEZ E, L TERRAY (2005). Large-scale atmospheric dynamics and local intense precipitation episodes. *Geophys Res Lett*, 32: L24711, doi:10.1029/2005GL023990.

SELTEN FM, G BRANSTATOR (2004). Preferred regime transition routes and evidence for an unstable periodic orbit in a baroclinic model. *J Atmos Sci*, 61: 2267-2268.

SLONOSKY VC, PD JONES, TD DAVIES (2000). Variability of the surface atmospheric circulation over Europe, 1774-1995. *Int J Climatol*, 20: 1875-1897.

STEPHENSON DB, A HANNACHI, A O´NEILL (2004). On the existence of multiple climate regimes. *Quart J Roy Meteor Soc*, 130: 583-605.

TRIGO RM, D POZO-VÁZQUEZ, TJ OSBORN, Y CASTRO-DÍEZ, S GÁMIZ-FORTIS, MJ ESTEBAN-PARRA (2004). North Atlantic oscilation influence on precipitation, river flow and water resources in the Iberian Peninsula. *Int J Climatol,* 24: 925-944.

UPPALA SM, PW KÅLLBERG, AJ SIMMONS, U ANDRAE, V DA COSTA BECHTOLD, M FIORINO, JK GIBSON, J HASELER, A HERNÁNDEZ, GA KELLY, X LI, K ONOGI, S SAARINEN, N SOKKA, RP ALLAN, E ANDERSSON, K ARPE, MA BALMASEDA, ACM BELJAARS, L VAN DE BERG, J BIDLOT, N BORMANN, S CAIRES, F CHEVALLIER, A DETHOF, M DRAGOSAVAC, M FISHER, M FUENTES, S HAGEMANN, E HÓLM, BJ HOSKINS, L ISAKSEN, PAEM JANSSEN, R JENNE, AP MCNALLY, JF MAHFOUF, JJ MORCRETTE, NA RAYNER, RW SAUNDERS, P SIMON, A STERL, KE TRENBERTH, A UNTCH, D VASILJEVIC, P VITERBO and J WOOLLEN (2005). The ERA-40 re-analysis. *Quart J Roy Meteor Soc,* 131: 2961-3012.doi:10.1256/qj.04.176.

VON STORCH H, FW ZWIERS (1999). Statistical Analysis in Climate research. Cambridge University Press, 510 pp.

WERNER PC, FW GERSTENGARBE, K FRAEDRICH, H OESTERLE (2000). Recent climate change in the North Atlantic European sector. *Int J Climatol,* 20: 463-471.

WILKS DS (2006). Statistical Methods in the Atmospheric Science. Academic Press, 627 pp.

YIOU P, M NOGAJ (2004). Extreme climatic events and weather regimes over the North Atlantic: When and where? *Geophys Res Lett,* 1: L07202, doi: 10.1029/2003GL019119.

ISBN: 978-84-8320-478-8

9 788483 201930

3,00 €
IVA incluido

GOBIERNO DE ESPAÑA
MINISTERIO DE MEDIO AMBIENTE Y MEDIO RURAL Y MARINO
AEMet
Agencia Estatal de Meteorología